Reconsideration of Case Histories for Estimating Undrained Shear Strength in Sandy Soils

C.E. (Fear) Wride[1], E.C. McRoberts[2] and P.K. Robertson[3]

Corresponding Author:

Dr. C.E. Wride
220 Civil/Electrical Engineering Building
University of Alberta
Edmonton, Alberta
CANADA, T6G 2G7

Phone: (403) 492-9646
Fax: (403) 492-8198
e-mail: cewride@civil.ualberta.ca

May 6, 1998
Submitted to the Canadian Geotechnical Journal

---

[1] Post-Doctoral Fellow, Geotechnical Group, Department of Civil and Environmental Engineering, University of Alberta, Edmonton, Alberta, Canada.

[2] Chief Technical Officer, AGRA Earth and Environmental Ltd., Edmonton, Alberta, Canada.

[3] Professor, Geotechnical Group, Department of Civil and Environmental Engineering, University of Alberta, Edmonton, Alberta, Canada.

Reconsideration of Case Histories for Estimating Undrained Shear Strength in Sandy Soils

C.E. (Fear) Wride, E.C. McRoberts and P.K. Robertson

Abstract

When sandy soils respond in a strain-softening manner to undrained loading, an estimation of the resulting undrained shear strength (S_u) is required to determine the potential for flow liquefaction at a given site. One of the most commonly used methods for estimating the undrained strength of liquefied sand is an empirical SPT-based chart (originally proposed by H.B. Seed), which was developed using a number of case histories. The original interpretations of these case histories are viewed by many workers and regulatory agencies as the most authoritative measure of the liquefied strength of sand. Consequently, in comparison, other less conservative methods are generally held in an unfavourable light. This paper re-examines the original database of case histories in view of some more recent concepts regarding soil liquefaction. The objectives of this paper are to explore and re-assess the issues involved in the original assessment and to offer alternative views of the case records. The conclusions presented here indicate that alternative explanations of the liquefied strength of sand are not inconsistent with the original case histories.

Key words: sandy soils, soil liquefaction, undrained strength, SPT

Introduction

If a sand is considered to be strain-softening (i.e. susceptible to flow liquefaction), an estimation of the resulting undrained shear strength (S_u) is required for stability analyses for either statically or dynamically triggered flow liquefaction. One of the most commonly used methods for estimating the undrained strength of liquefied sand is the SPT-based chart by Seed and Harder (1990), based on earlier work by Seed (1987). The chart is based on 17 case histories and provides a relationship between S_u and equivalent normalized Standard Penetration Test (SPT) resistance, $(N_1)_{60}$, in clean sand. Figure 1 presents a metric version of the Seed and Harder (1990) chart, identifying the case histories by number. Table 1 summarizes the data presented in Figure 1, in tabular form.

Several issues arise in practice when using this relationship, which is considered by many to be the most authoritative standard for assessing the undrained strength of liquefied soil. First, there are other techniques available for assessing the undrained strength of loose sand (e.g. Byrne et al., 1994; Fear and Robertson, 1995; Konrad and Watts, 1995; Yoshimine et al., 1998) which often result in higher design strengths for denser soils than those predicted by Figure 1. Second, practice often results in a lower bound assessment of the lowest $(N_1)_{60}$ for a given site or soil unit and the subsequent introduction of this value into the lower bound relationship given in Figure 1. As will be shown, the selection of the $(N_1)_{60}$ values in the original interpretation of the case histories often did not adopt a lower bound of the in-situ $(N_1)_{60}$. Therefore, a considerable degree of potentially unwarranted conservatism can be introduced when Figure 1 is applied in practice. Thirdly, Fear and McRoberts (1995) reviewed the database compiled by Seed et al. (1984) and presented an alternative assessment of the seismic triggering of sands using a lower bound

assessment of the site data. The conclusion was that triggering was not observed above an $(N_1)_{60}$ of about 15. Therefore, it can be suggested that the prediction offered by Figure 1 (i.e. that a sand with $(N_1)_{60} > 15$ may have a strain-softening response and a low undrained shear strength) may well be unlikely. Finally, it is possible that some of the case histories are cases of true flow liquefaction for which S_u is meaningful; however, some of the case histories appear to be cases of cyclic liquefaction for which deformations might be associated with a loss in soil stiffness rather than a loss in soil strength (Robertson, 1994).

The intent of this paper is to provide a review of the original case records in order to consider if an alternative view – and one more supportive of other developments in liquefaction – could be seen in the original database. The review of the database presented in this paper assesses the case histories on a somewhat qualitative basis. A full discussion of the database is provided in one chapter of the first author's Ph.D. dissertation (Fear, 1996). Further studies into each of the individual case histories would be both interesting and useful in an attempt to answer some of the questions that are raised here and to assess the case histories in a more quantitative manner.

Historical Information about the Case Histories

Essential statistics

Table 2 summarizes some essential statistics for each of the individual case histories. Included in Table 2 are the 17 case histories from the original database by Seed and Harder (1990), three case histories added to the database by Stark and Mesri (1992) and an additional case history, Duncan Dam (Byrne et al., 1994). The case histories are identified by name and number. The numbers were used to identify the case histories in Figure 1 and are used in subsequent figures throughout

this paper. Included in Table 2 for each case history are the initial height and slope angle, the type of trigger mechanism, the earthquake (EQ) magnitude and acceleration (if applicable), the nature of the observed failure, the runout distance (defined as the horizontal distance from the toe of the original slope to the toe of the post-failure slope) and the post-failure slope angle.

Other key facts

Detailed descriptions of each of the case histories are provided by Fear (1996), based on the work by Seed (1987), Seed and Harder (1990) and Stark and Mesri (1992) as well as the many original references for each case history. Thus, these descriptions will not be repeated here. However, several key facts will be emphasized, as outlined in Table 3 and described below. References for each case history in addition to the three main papers are cited in Table 3.

As indicated in Table 3, the various failures occurred between 1918 and 1987. Nine of the failures occurred prior to 1970. It is likely that the data for older case histories may be less reliable than those for more recent failures. A related fact is that there were no SPT data available for most of the failures which occurred prior to 1970; only limited data were available for the Fort Peck Dam case history. For two of the later case histories, only Becker penetration test (BPT) data or cone penetration test (CPT) data were available. In the case of the Lower San Fernando Dam, only post-earthquake downstream SPT data were available; using various assumptions, these data were extrapolated to pre-earthquake upstream SPT data. Therefore, for many case histories, values of $(N_1)_{60}$ can only be estimated and, as a result, are less reliable. In addition, as indicated in Table 3, both the Lower and Upper San Fernando Dams consisted of highly stratified deposits. In such materials, selecting a representative $(N_1)_{60}$ is very difficult.

For each case history, Table 3 also indicates the type of structure involved, the direction of the failure, whether the failure involved a mass of soil or a distinct layer of soil, and various other observations regarding the nature of some of the failures, as reported in the literature. Consequently, the table is useful for identifying some additional similarities and differences between the various case histories.

The additional case history presented here is Duncan Dam. Duncan Dam is a hydroelectric dam located on the Duncan River, about 8 km upstream from Kootenay Lake in southeastern British Columbia, Canada. The dam itself has never experienced a liquefaction failure; however, a recent dam safety review by B.C. Hydro (Little et al., 1994) investigated the seismic resistance of the dam, with liquefaction resistance of primary concern. Duncan Dam is a zoned earthfill embankment founded on sandy soils. In-situ testing and sampling (Sego et al., 1994; Plewes et al., 1994), laboratory testing of undisturbed frozen samples (Pillai and Stewart, 1994) and subsequent analysis (Pillai and Salgado, 1994) indicated that the soil unit of greatest concern was Unit 3-c, which is located under the downstream side of the right half of Duncan Dam. Unit 3-c consists of uniform fine sand with approximately 5% fines. The sand is composed of angular to subangular grains of quartz, plagioclase, K-feldspar and calcite-dolomite.

Representative values of $(N_1)_{60}$ and S_u selected by other authors

Over the years, different researchers have assigned different representative values of $(N_1)_{60}$ and S_u to each case history in the Seed and Harder (1990) and Stark and Mesri (1992) databases. These values are summarized in Table 4 and Table 5, together with comments as to how they

were selected by the various authors.

At Duncan Dam, the in-situ site investigation found that the SPT $(N_1)_{60}$ increased non-linearly with increasing overburden stress (Byrne et al., 1994; see Table 6). Laboratory testing (post-cyclic undrained monotonic simple shear tests) of undisturbed frozen samples concluded that an undrained residual shear strength ratio, S_u/σ'_{vo}, of 0.21 was applicable to the Unit 3-c sand (Pillai and Salgado, 1994). As shown in Table 6, the site investigation and laboratory testing results for Duncan Dam can be combined, in order to correlate values of S_u with values of $(N_1)_{60}$ for given values of overburden pressure. These datapoints can be plotted and compared with the other empirical case histories discussed above, keeping in mind that this case history did not fail.

Classification of the Case Histories

Summary of case history statistics

As mentioned earlier, Table 2 summarizes essential details for each of the individual case histories. Based on the details in Table 2 and the information presented earlier, the case histories in Table 2 have been classified into various categories in an attempt to ultimately distinguish between cases of flow liquefaction (strain-softening response) and cyclic liquefaction. Of the 21 case histories listed in Table 2, three case histories were statically triggered failures, while 17 case histories suffered some type of deformations as a result of cyclic loading. The cyclic loading was predominantly earthquake loading, but one case history (18, Lake Ackerman) was triggered by cyclic loading related to a seismic exploration. The type of failure assigned to each case history in Table 2 will be discussed below.

Comparison of initial conditions

Table 2 clearly indicates that the database contains a wide range of initial slope height and angle combinations. Five case histories had initial slope angles less than 5° (this includes case history 6, which was not a slope, but a building on level ground). Of these five case histories, only case history 10 (San Fernando Juvenile Hall) has a large slope height (i.e. > 10 m). As explained in Table 2, this is a result of the fact that the lateral spread at the site was approximately 1.2 km long and thus there was a 30 m height difference between the toe and head of the slide mass area. Eight case histories had initial slope angles greater than 25°, but all of these case histories had initial slope heights of less than 11 m. Nine case records had initial slope angles ranging from approximately 11° to 22°. Although one of these case records (2, Sheffield Dam) had an initial slope height of 7.6 m, the others had much higher initial slope heights ranging from 17.6 to 61 m.

Comparison of observed deformations

Drawing on the information in Table 1 and Table 2, Table 7 provides a summary of the simple deformation analysis performed as part of this study. For each of the case histories, several terms have been computed to help quantify the observed deformations relative to those experienced by the other case histories in the database.

The observed runouts for the various case histories cannot be compared directly because of the wide range in initial slope height (see Table 2). It is logical to conclude that as the initial slope height increases, observed runouts could increase as a result of the higher driving stresses and the additional momentum that the material will gather as it fails. Dividing the observed runout by

the initial slope height provides a simple way of comparing relative runouts between various case histories. Table 7 indicates that nine of the case histories had relative runouts of 3 or greater. The remaining case histories had relative runouts ranging from zero to 2. A related term to the relative runout ratio is the amount of horizontal strain that occurred. This was defined by simply dividing the observed runout by the initial slope length (defined as the horizontal distance from the toe of the initial slope to the point immediately below the crest of the initial slope) and expressing the result in percent. Table 7 indicates that eleven of the case histories had horizontal strains greater than 90%. Four of the case histories had horizontal strains less than 4%.

Another simple measure for comparing the deformations of the various case histories is the relative slope ratio. This is defined as the ratio of the post-failure slope angle to the initial slope angle. Table 7 indicates that four of the case histories had relative slope ratios of 1.0; i.e. no significant change in slope was observed from before to after the soil failure. Ten case histories had relative slope ratios of less than 0.40. Figure 2 indicates that there is a clear relationship between relative runout and relative slope angle for all of the case histories. This is to be expected because a slope that runs out further relative to its initial height would obviously have a lower ratio of its post-failure slope angle to its initial slope angle. However, as will be discussed further in later sections of this paper, what is of most interest is where the various case histories happen to plot in Figure 2.

Another method of comparing the various failures is in terms of brittleness index (I_B). Sladen et al. (1987) suggested that for slides that do not involve toe erosion, the brittleness index of the slope failure can be estimated by comparing initial and post-failure slope profiles using the following formula:

[1] $$I_B = \frac{\tan\beta_i - \tan\beta_f}{\tan\beta_i}$$

where β_i and β_f are the initial and post-failure slope angles, respectively. This term is related to the relative slope ratio term discussed above. Note that the maximum possible value for I_B using Equation 1 is 1.0. Table 7 indicates that ten of the original Seed and Harder (1990) case histories have values of I_B greater than or equal to 0.64.

Sladen et al. (1985b) found that the brittleness index of a soil in undrained loading appears to be related to the state of a sandy soil, when measured in terms of the ratio of the initial mean normal effective stress of the soil to that at steady state at the same void ratio. Fear (1996) used the same measure of state for sandy soils and termed it reference state ratio (RSR). RSR is given by the following formula:

[2] $$RSR = \frac{p'_i}{p'_{us}}$$

where p'_i is the initial mean normal effective stress and p'_{us} is the mean normal effective stress at ultimate (steady) state at the same void ratio. Note that p'_{us} is related to the deviator stress at ultimate state, q_{us}, by the following formula:

[3] $$M = \frac{q_{us}}{p'_{us}}$$

Estimating the average RSR for each case history is difficult. The best that can be done is to calculate an approximate single average value. The average value of p'_i was estimated based on the average value of σ'_{vo} given by Stark and Mesri (1992) for the middle of the liquefied layer and assuming a K_o of 0.5. The average value of p'_{us} was estimated by assuming an average M of 1.2 (which, for triaxial compression loading, corresponds to ϕ'_{us}=30°), assuming that $q_{us} = 2S_u$, and using the mean value of S_u in the Seed and Harder (1990) database. Clearly, the resulting average RSR is only an estimation and may be somewhat inaccurate. Nevertheless, it is interesting to compare the relationship between I_B and estimated RSR for the case histories in the original Seed and Harder (1990) database (with the exception of case history 2, for which the post-failure angle was not available, and case history 6, which was not a slope failure) with that suggested by Sladen et al. (1985b), as presented in Figure 3. Despite some scatter, there is definitely an observable increase in I_B with increasing RSR, similar to that suggested by Sladen et al. (1985b). The only exceptions to this are the lateral spread case histories (8, 10, and 14), which have zero brittleness irrespective of the estimated RSR because no significant change in slope angle occurred as a result of each lateral spread.

Classification based on deformation characteristics

In general, as outlined in Table 2, all of the case histories in the database can be divided into three types of failures: flow failures, slump failures and lateral spreads. The category that a given case history falls into depends on its deformation characteristics as quantified by the various terms in Table 7. Case histories in the database classified as flow failures have large relative runouts (and large strains) and small slope angle ratios (and large values of I_B). As an

example, Figure 4(a) illustrates the flow failure at the Calaveras Dam (case history 1). Case histories in the database classified as lateral spreads have small relative runouts (and small strains), slope angle ratios of 1.0 (and I_B values of zero) and occur in gently sloping ground (i.e. initial slope angle $\leq 5°$). As an example, Figure 4(b) illustrates the lateral spread at Whiskey Springs Fan (case history 14). Slump failures have deformation characteristics in between those of flow failures and those of lateral spreads. Case histories in the database classified as slump failures have smaller relative runouts (and smaller strains) and larger slope angle ratios (and smaller values of I_B) than the flow failures, but have large enough deformations in steeply sloping ground that they cannot be considered to be lateral spreads. As an example, Figure 4(c) illustrates the upstream and downstream slump failures at La Marquesa Dam (case records 15 and 16, respectively). The large deformations could have resulted from cyclic liquefaction combined with large earthquake motions.

This study has classified flow failures as those failures which had a relative runout of 2 or greater and a slope angle ratio of less than 0.4. Therefore, case histories 1, 3, 4, 7, 9, 13a & b, and 19 (Calaveras Dam, Fort Peck Dam, Solfatara Canal Dike, Uetsu Embankment, Mochi-Koshi Tailings, and Nerlerk Embankment, respectively) would be classified as flow failures (see data in Figure 2). Case histories 8, 10, and 14 (Snow River Bridge Fill, San Fernando Juvenile Hall, and Whiskey Springs Fan, respectively) would be classified as lateral spreads because they all had a relative runout less than 2, a slope angle ratio of 1 and occurred in gently sloping ground (initial slope angle $\leq 5°$). Case histories 5, 12, 15, 16 and 17 (Lake Merced Bank, Upper San Fernando Dam, La Marquesa Dam - Upstream and Downstream, and La Palma Dam, respectively) would be classified as slump failures because they had relative runouts less than 2 and slope angle ratios greater than 0.4. Case histories 11 and 18 (Lower San Fernando Dam and Lake Ackerman,

respectively) can be considered as borderline between the flow and slump categories.

The dividing line between a flow failure and a slump failure, as described above, is obviously somewhat subjective. It would be reasonable to expect some transition zone between flow and slump type failure deformation characteristics. Examining Figure 3, the dividing line between flow and slump failures in terms of brittleness index is an I_B of about 0.6. It is interesting to note that the classification of the individual case histories is similar to that by Baziar and Dobry (1995) who divided the database into flow slides, lateral spreads and major slides.

Flow Liquefaction versus Cyclic Softening

Robertson and Fear (1995), building on earlier work by Robertson (1994), proposed specific definitions of soil liquefaction, which distinguished between flow liquefaction (strain-softening response in undrained loading initiated by either a monotonic or cyclic trigger mechanism) from cyclic softening (progressive decrease in soil stiffness during cyclic loading). Cyclic softening was further divided into cyclic liquefaction (shear stress reversal occurs and zero effective stress can be reached) and cyclic mobility (no shear stress reversal occurs). A full description of these definitions is given by Robertson and Wride (1998) in a recent NCEER report on soil liquefaction evaluation (NCEER, 1998). It is often difficult, if not impossible, to distinguish between flow liquefaction (strain-softening response) and cyclic softening (liquefaction) phenomena in the field after a failure has occurred. Both types of liquefaction can result in large deformations. Ideally, instrumentation during and after a failure together with comprehensive site characterization would be required to correctly identify which phenomenon occurred. However, such information is not available for the case histories being discussed here. The best

that can be done is to make an estimate of which phenomenon controlled which case history, based on the terminology definitions described above and the observed deformation characteristics of each case history.

Statically triggered slope failures

Case histories 1 (Calaveras Dam), 3 (Fort Peck Dam), and 19 (Nerlerk Embankment) suffered failures as a result of static triggers. All three of these case histories have been classified as flow failures. Provided that failure truly occurred in the sand within each slope, these three case histories would have to be classified as cases of flow liquefaction, because the trigger was static. As indicated in Table 3, there is some ongoing debate over the influence of other factors such as weak clay shale or clay layers influencing the failure. However, it is possible that although strains may have first occurred in these weak layers, they may have been sufficiently large to trigger flow liquefaction in the strain-softening sand above, such that the overall failure was a result of the phenomenon of flow liquefaction.

Cyclically loaded case histories

Of the case histories in Table 2, one case history (21, Duncan Dam) did not fail, but consisted of field and laboratory studies investigating what conditions could lead to failure. Case history 6 (Kawagishi-Cho Building) differed from all of the other cyclically loaded case histories in that it consisted of the failure of a building foundation rather than deformations or failure of a slope. However, the remaining 16 case histories suffered some type of slope deformation as a result of cyclic loading. As discussed in the previous section, these case histories have been subdivided as to the nature of the deformation that occurred (see Table 2).

Lateral spreads

Four of the cyclically loaded case histories (8, 10, 14 and 20; Snow River Bridge Fill, San Fernando Juvenile Hall, Whiskey Springs Fan, and Heber Road, respectively) were lateral spreads, rather than severe slope failures. All four of these case histories had initial slope angles less than or equal to 5° and suffered no significant change in slope angle after failure. Each of these case histories suffered lateral deformations ("runouts") of less than or equal to 3 m. Youd (1993), based on earlier work by Bartlett and Youd (1992) included all four of these case histories within a database of lateral spread case histories. Since these lateral spreads occurred in level to gently sloping ground, it is reasonable to conclude that shear stress reversal did occur during the earthquake loading. Consequently, these lateral spreads are all likely deformations that are predominantly a result of cyclic softening (liquefaction).

Flow failures

Case histories 4, 7, 9, and 13a &b (Solfatara Canal Dike, Uetsu Embankment, Mochi-Koshi Tailings Dam 2 and Dam 1, respectively) were all cyclically loaded case histories that were classified as flow failures (see Figure 2). It is likely that these case histories suffered such large runout ratios and responded in such a brittle manner because they contained a sufficiently large mass of potentially strain-softening material that was triggered to strain-soften by the cyclic loading. Once triggered, the driving stresses were higher than the undrained shear strength and the material flowed significantly relative to the size of the slope or embankment. Thus, these case records are likely all cases of flow liquefaction. They can be grouped together with the statically triggered cases of flow liquefaction discussed earlier.

Slump failures

The slump failures are more difficult to classify as being controlled primarily by either flow liquefaction or cyclic softening (liquefaction). The observed slumping deformation pattern could be due to either type of liquefaction. If flow liquefaction occurred within the soil structure, there must have been an insufficient quantity of strain-softening material relative to strain-hardening material to result in a true flow failure. However, if shear stress reversal did occur within the soil structure, cyclic liquefaction with deformations accumulating during cyclic loading may have caused the observed deformations. In particular, if cyclic liquefaction occurred in the level ground at the toe of any of the slopes, the slumping deformation pattern may have been a result of the soil structure moving into the zone of softened soil. Further studies into all of the failures would be required to clearly identify what happened at each site. However, for interest, this study attempts to distinguish between possible flow liquefaction and possible cyclic softening.

Using results by Pando and Robertson (1995) as a guide, it is possible that shear stress reversal may have occurred within the slope of case histories 5, 15, 16 and 17 (Lake Merced Bank, La Marquesa Dam - Upstream and Downstream, and La Palma Dam, respectively) because they were all relatively short steep structures (see Table 2). In particular, shear stress reversal may have occurred in the level ground in the toe region of each slope, causing a loss in soil stiffness and resulting in the embankment slumping into the surrounding ground. Case history 6 (Kawagishi-Cho Building) may have been affected by a similar phenomenon.

Case history 12 (Upper San Fernando Dam) was a large enough structure that it is possible that

shear stress reversal may not have occurred throughout the structure. A more probable explanation is that the dam consisted of a small portion of strain-softening or limited strain-softening material such that it suffered damaging, but limited deformations, rather than a catastrophic flow failure. The presence of the downstream berm may have also contributed to limiting the deformations that occurred.

Case histories 11 and 18 (Lower San Fernando Dam and Lake Ackerman, respectively) which were considered as borderline between the flow and slump categories, may have contained more strain-softening material than case history 12, but still had an insufficient amount to result in relative runouts as high as most of the flow failure case histories. Also, the approximate RSR for the Lower San Fernando Dam was smaller than the approximate values of RSR calculated for the other case histories classified as flow failures (i.e. it appears to have had a denser initial state than the other flow failure case histories; see Table 7). Nevertheless, these two case histories will be included with the flow failure group because the deformations were fairly large and their slope angle ratios were low. The observation of a time delay between the end of the earthquake and the failure of the Lower San Fernando Dam supports the classification of the case history as flow liquefaction. However, the zone of material that suffered flow liquefaction was limited in size relative to the overall size of the dam, resulting in the borderline flow/slump deformations.

S_u versus $(N_1)_{60}$ for flow liquefaction case histories

Figure 5 presents a similar plot to that by Seed and Harder (1990) given in Figure 1, but includes only the case histories in the combined Seed and Harder (1990) and Stark and Mesri (1992) database which were classified as flow failures or borderline flow/slump failures (see Table 2).

These case histories are considered most likely to be cases of flow liquefaction, for which estimating an undrained strength is appropriate. Clearly, the data still falls within the Seed and Harder (1990) boundary lines because the values of S_u and $(N_1)_{60}$-cs have not been changed. However, it is important to note that case histories 1, 2, 3, 4, and 7 had SPT values which were only estimated because little or no data were available (see Table 3 and Table 4). Therefore these data contain uncertainty; in particular, case histories 1 and 3, which have higher SPT values can be considered to have larger uncertainty associated with them than the lower blowcount case histories. Case history 19 had SPT values estimated from CPT measurements. Case history 11 consisted of highly interbedded silt and sand layers; hence, the average SPT blowcount can be misleading. If case histories 1, 3, 11 and 19 are removed from the plot because of the uncertainty associated with their SPT values, no case history data for flow failures are left with values of SPT $(N_1)_{60}$-cs > 6. Hence, the shape of the relationship for $(N_1)_{60}$-cs > 6 becomes uncertain.

Superimposed on Figure 5 is a theoretical ultimate state strength line (for triaxial compression direction of loading) for clean Ottawa sand (K_o=0.5), based on the results of Fear and Robertson (1995). Also superimposed on Figure 5 are the results from the detailed site investigation and laboratory testing for case record 21 (Duncan Dam), as summarized in Table 6. The sand under investigation at Duncan Dam was essentially a clean sand, having a fines content of 5 to 8%. Consequently, essentially no blowcount correction is required for fines content and the measured $(N_1)_{60}$-in-situ values can be plotted directly on this figure. The data for Duncan Dam (which did not fail) certainly appear to follow the trend of the theoretical lines for Ottawa sand loaded in triaxial compression. For values of $(N_1)_{60}$-cs greater than about 10, both the Ottawa sand line and the Duncan Dam data certainly suggest a different trend to the relationship between S_u and $(N_1)_{60}$-cs than that suggested by the Seed and Harder (1990) boundary lines.

Representative Values of $(N_1)_{60}$ and S_u

Range of data reported in the literature

Table 1 summarized the values of $(N_1)_{60}$ (both in-situ and clean sand equivalent) and S_u used by Seed and Harder (1990). However, there is considerable uncertainty in the selected values and there appears to be a wide range of reported representative values of $(N_1)_{60}$ and S_u for each case history (as indicated in Table 4 and Table 5).

It is important to note, as outlined earlier (see Table 3), that several of the case histories in the Seed and Harder (1990) database had representative $(N_1)_{60}$ values selected based on no or little SPT data. In particular, case histories 1 and 3 (Calaveras Dam and Fort Peck Dam), which are two of the case histories with higher representative values of $(N_1)_{60}$ (see Figure 1), had $(N_1)_{60}$ values assigned based on relative density type estimates. Case history 16 (La Marquesa Dam, Downstream Slope), which was also one of the higher $(N_1)_{60}$ case histories (see Figure 1), appears to have a representative $(N_1)_{60}$ selected based on a single blowcount in the layer that appeared to have liquefied. Case history 14 (Whiskey Springs Fan had SPT values estimated from Becker penetration test (BPT) measurements. Case history 19 had SPT values estimated from CPT measurements. Uncertainties also arise for case histories 11 and 12 (Lower and Upper San Fernando Dams, respectively) which had the highest representative $(N_1)_{60}$ values in the Seed and Harder (1990) database (see Figure 1). The selected values were extrapolated from post-earthquake conditions to pre-earthquake conditions and in the case of the Lower San Fernando Dam, from downstream conditions to upstream conditions. In addition, the

interbedded nature of the case history 11 and 12 deposits make the selection of an appropriate blowcount value difficult. Some of the uncertainties associated with the selection of representative values of S_u are discussed later in this paper.

Table 8 summarizes the range in values of $(N_1)_{60}$-in-situ, S_u and estimated fines content, as reported by various authors and given in Table 4 and Table 5. Based on the estimated fines content, the values of $(N_1)_{60}$-in-situ could be converted to equivalent clean sand values of $(N_1)_{60}$-cs (after Seed, 1987). It is important to note that there is a considerable uncertainty with these fines content corrections. The data given for the case histories in Table 8 clearly cover a wider range than in Table 1, based on the Seed and Harder (1990) data alone.

A minimum $(N_1)_{60}$ approach

In general, the values of $(N_1)_{60}$ in the Seed and Harder (1990) chart appear to be average representative values for each case history. Experience has shown that the Seed and Harder (1990) chart often gives conservative estimates of S_u (e.g. Byrne et al., 1994), particularly when applied to all points in an SPT profile, including any low values. Based on the discussion in Fear and McRoberts (1995), it is likely the "weakest-link-in-the-chain", represented by the minimum $(N_1)_{60}$, that can result in either cyclic softening (liquefaction) or flow liquefaction being triggered at a particular site. Likewise, it could be argued that the resulting estimation of undrained shear strength for a liquefied soil deposit should be correlated with the minimum representative $(N_1)_{60}$, rather than the average value. Based on earlier work by Popescu (1997), Yoshimine et al. (1998) suggested that the 80-percentile value, or approximately the mean minus one standard deviation, of CPT data would be the appropriate value to link to undrained shear

strength. Since CPTs are continuous in nature and, particularly if several CPTs are conducted adjacent to one another, this calculation is fairly straightforward. However, when only limited SPT data are available, calculating a representative mean minus one standard deviation of $(N_1)_{60}$ is difficult. Therefore, selecting the minimum $(N_1)_{60}$ value may be a reasonable alternative.

Table 9 presents a summary of the revised values of S_u and $(N_1)_{60}$ chosen to represent each case history, based on the minimum $(N_1)_{60}$ viewpoint. A reasonable lower bound $(N_1)_{60}$-in-situ was selected and the clean sand equivalent value was estimated based on the fines content and the SPT corrections proposed by Seed (1987). Table 9 provides comments regarding the selection of both S_u and $(N_1)_{60}$ for each case history. When possible, the value of S_u was selected as one which incorporated energy effects (Poulos, 1988; Davis et al., 1988), as this was felt to be closer to the "true" value of S_u. Conducting this exercise led to the conclusion that it is very difficult to represent a complex slope failure by a single S_u and a single $(N_1)_{60}$.

Although Table 9 presents the revised selections of S_u and $(N_1)_{60}$ for each of the case histories in the database, an undrained shear strength is really only appropriate for cases of flow liquefaction. While cases of cyclic softening (liquefaction) will likely experience deformations related to the minimum $(N_1)_{60}$, undrained shear strengths are not appropriate to the analysis of such a site. At best, they can represent equivalent values of S_u that would result in similar deformations as those caused by the progressive loss in soil stiffness. However, these values of S_u may not be appropriate for analyzing sites outside of the database.

Figure 6 presents the revised selection of S_u and $(N_1)_{60}$-cs in Table 9 for the case histories in the combined Seed and Harder (1990) and Stark and Mesri (1992) database that were classified as

flow failures and borderline flow/slump failures. Superimposed on Figure 6 are the Seed and Harder (1990) boundary lines and the K_o=0.5 theoretical line for clean Ottawa sand (Fear and Robertson, 1995). The general trend of the data appears to be more similar to the clean Ottawa sand line than the Seed and Harder (1990) boundary lines. However, the data are fairly limited and contain considerable scatter. If case histories 1, 3, 11 and 19 are removed due to the larger uncertainty in their SPT data, the shape of the relationship for $(N_1)_{60}$-cs > 6 becomes uncertain.

The earlier discussion has suggested that undrained shear strengths only have real meaning for flow liquefaction case histories. Although an attempt has been made here to separate what appear to be true flow failures from other case histories in the database, some uncertainty remains as to which case histories should actually be included on a plot of S_u versus $(N_1)_{60}$-cs. Therefore, Figure 7 presents the same plot as in Figure 6, but with all of the case histories shown, rather than just what are considered here to be true flow failures. Different symbols are used to distinguish each type of failure; i.e. flows and flow/slumps, slumps, lateral spreads, and the one building failure. Case history 5 (Lake Merced) is not shown in Figure 7 because an argument has been made in this study to remove it from the database (see Table 3 and Table 4). Similar conclusions can be drawn for Figure 7 as were drawn above for Figure 6.

Figure 8 presents the same data as in Figure 7, but in terms of undrained shear strength ratio. In order to normalize the values of undrained shear strength used in Figure 7, the values of σ'_{vi} selected by Stark and Mesri (1992) were used for each case history (see Table 7). However, for the Nerlerk Embankment case history (19), the value of S_u/σ'_{vi} of 0.148 selected by Stark and Mesri (1992) was used directly (see Table 5). Most of the flow failure case histories had values

of S_u/σ'_{vi} of less than 0.15. No data plot above an $(N_1)_{60}$-cs of 10. However, in general, the data appear to suggest a different trend than that suggested by the Stark and Mesri (1992) boundary lines, which are shown in Figure 8 for comparison. Also shown for comparison K_o=0.5 theoretical line for clean Ottawa sand (Fear and Robertson, 1995).

Uncertainty with S_u

In reviewing the case histories in the combined Seed and Harder (1990) and Stark and Mesri (1992) database, it soon becomes clear that there is considerable uncertainty in the selection of a representative value of S_u for an individual case history (see Table 4 and Table 5). As indicated in Table 3, many of the case histories involved "liquefaction" of a soil mass, while others (case histories 2, 10, 15, 16, 17, 18 and 20) involved "liquefaction" of a particular soil layer. For case histories involving failure of a soil mass, the zone occupied by the mass within the soil structure was sometimes limited in extent (e.g. case histories 11 and 12). Different assumptions were made by various authors as to the mechanics of failure in calculating a single representative S_u for each case history, resulting in the range of reported values presented in Table 8. For example, Lucia (1981) and Lucia et al. (1982) calculated S_u based on post-failure slope configurations, while Poulos (1988) and Davis et al. (1988) noted that the pre-failure and post-failure driving stresses would bracket the actual mobilized undrained shear strength and attempted to account for energy effects associated with the dynamics of failure when calculating the values of S_u.

In actual fact, a single value of S_u may reflect only the overall failure, but not apply everywhere within the failing soil mass or layer. Different directions of loading may occur at different points

within a soil structure such that various elements reach different values of S_u. However, many authors assume a single S_u along a failure surface. In addition, variability in soil state within the soil mass could result in different elements of soil having different values of S_u. Some failures (e.g. 19, Nerlerk embankment) were progressive in nature. If this is not accounted for, undrained strengths may not be properly estimated. Newmark type deformation analyses were often used to estimate the S_u that would result in the observed accumulated deformations during cyclic loading for the lateral spreading type case histories. However, the previous discussion has suggested that these deformations are generally due to a loss in soil stiffness during cyclic loading. While a value of S_u estimated using this method may match the observed deformations at a particular site, it is really only an equivalent S_u because the physics leading to failure did not necessarily involve a loss in strength. Extrapolating such results to other sites is not appropriate.

Deformations that result from the phenomenon of cyclic softening (liquefaction) should not be analyzed using an undrained shear strength in a stability analysis. Although the magnitude of the deformations that may occur will depend on the density of the soil (as indicated by $(N_1)_{60}$ values), they will also depend on the size and duration of cyclic loading. Other methods such as that developed by Youd (1993) should be used to estimate deformations associated with potential lateral spreads. Sloping ground that is not considered to be susceptible to flow liquefaction based on site specific testing should be carefully evaluated for the potential of cyclic softening (liquefaction) and resulting deformations. In such cases, it is important to carefully evaluate the level ground at the toe of a slope, in order to examine the effect that cyclic liquefaction and loss in stiffness within that zone may have on overall deformations of the slope. Similar investigations should be carried out for buildings located on level ground.

Conclusions

The empirical SPT-based chart by Seed and Harder (1990) is one of the most commonly used methods for estimating the undrained shear strength of sand for either statically or dynamically triggered flow liquefaction. This paper has illustrated the complexity and range of liquefaction failures contained within the combined Seed and Harder (1990) and Stark and Mesri (1992) database. It appears that the database contains a wide range of deformation characteristics and possibly a variety of flow liquefaction and cyclic softening case histories. However, after a failure has occurred, it is often very difficult to correctly identify which phenomenon controlled the observed deformations. In addition, the detailed summaries provided for each case history illustrate the difficulty in assigning a single S_u and a single $(N_1)_{60}$ to a complex slope failure.

Recent studies (e.g. Byrne et al., 1994; Fear and Robertson, 1995; Konrad and Watts, 1995; Yoshimine et al., 1998) have indicated that the undrained shear strength of sand is a flow liquefaction response parameter that is very sensitive to variability in a soil deposit as well as the direction of loading. These approaches often result in higher design strengths for denser soils than those predicted by the Seed and Harder (1990) chart. Nevertheless, the Seed and Harder (1990) chart continues to be considered by many workers and regulatory agencies as the most authoritative standard for assessing the undrained strength of liquefied soil.

However, the original relationships proposed by Seed and Harder (1990) appear to be conservative and based on average representative $(N_1)_{60}$ values for each case history. As a result, when applied in practice, they may be overly conservative for low points in any SPT $(N_1)_{60}$

profile in a soil deposit. In addition, the original database appears to contain limited reliable data for $(N_1)_{60}$-cs > 6; thus, the shape of the relationship between S_u and $(N_1)_{60}$-cs becomes uncertain. However, as suggested by other authors (e.g. Byrne et al., 1994; Konrad and Watts, 1995; Fear and Robertson, 1995; Yoshimine et al., 1998), the relationship may be extremely sensitive to small changes in density at values of $(N_1)_{60}$-cs in the order of 10 to 15. When $(N_1)_{60}$-cs falls above this threshold value, undrained strengths may be quite large. This is consistent with Fear and McRoberts' (1995) observation that a lower bound assessment of the Seed et al. (1984) seismic triggering database showed that seismic triggering was not observed above an $(N_1)_{60}$ of about 15.

Finally, when re-examined in view of some of the more recent concepts regarding soil liquefaction, it appears that the case histories in the original database are not inconsistent with alternative views and other recent developments in liquefaction. Thus, in practice, the revised database could be a useful tool which should be used in conjunction with other alternative approaches when assessing a particular site for instability due to flow liquefaction. The review of the database presented here assessed the case histories on a somewhat qualitative basis. Further studies into each of the individual case histories would be both interesting and useful in an attempt to answer some of the questions that are raised here and to assess the case histories in a more quantitative manner.

References

Andrus, R.D. and Youd, T.L. 1987. Subsurface investigation of a liquefaction induced lateral spread - Thousand Springs Valley, Idaho. *Report prepared for the U.S. Army Corps of Engineers (miscellaneous paper GL-87-8)*, Department of Civil Engineering, Brigham Young University, Provo, Utah.

Andrus, R.D., and Youd, T.L. 1989. Penetration tests in liquefiable gravels. *Proceedings of the 12th International Conference on Soil Mechanics and Foundation Engineering*, Rio de Janeiro, 1: 679-682.

Andrus, R.D., Youd, T.L., and Carter, R.R. 1986. Geotechnical evaluation of a liquefaction induced lateral spread, Thousand Springs Valley Idaho. *Proceedings of the 22nd Annual Symposium on Engineering Geology and Soils Engineering*, Boise, ID, February 24-26, 1984.

Bartlett, S.F., and Youd, T.L. 1992. Empirical analysis of horizontal ground displacement generated by liquefaction-induced lateral spread. *National Center for Earthquake Engineering Research, Technical Report NCEER-92-0021.*

Baziar, M.H., and Dobry, R. 1995. Residual strength and large-deformation potential of loose silty sands. *Journal of Geotechnical Engineering*, ASCE 121(12): 896-907.

Been, K., Crooks, J.H.A., Becker, D.E., and Jefferies, M.G. 1986. The cone penetration test in sands: part I, state parameter interpretation. *Géotechnique*, 36(2): 239-249.

Been, K., Conlin, B.H., Crooks, J.H.A., Fitzpatrick, S.W., Jefferies, M.G., Rogers, B.T., and Shinde, S. 1987a. Back analysis of the Nerlerk berm liquefaction slides (Discussion). *Canadian Geotechnical Journal*, 24: 170-179.

Been, K., Jefferies, M.G., Crooks J.H.A., and Rothenburg, L. 1987b. The cone penetration test in sands: part II, general inference of state. *Géotechnique*, 37(3): 285-299.

Bennett, M.J. 1989. Liquefaction analysis of the 1971 ground failure at the San Fernando Valley Juvenile Hall, California. *Bulletin of the Association of Engineering Geologists*, 26(2): 209-226.

Byrne, P.M., Imrie, A.L., and Morgenstern, N.R. 1994. Results and implications of seismic performance studies for Duncan Dam. *Canadian Geotechnical Journal*, 31:-979-988.

Casagrande, A. 1965. Role of the 'calculated risk' in earthwork and foundation engineering. The Terzaghi Lecture, *Journal of the Soil Mechanics and Foundations Division*, Proceedings of the ASCE, 91(SM4): 1-40.

Davis, Jr., A.P., Castro, G. and Poulos, S.J. 1988. Strengths backfigured from liquefaction case histories. *Proceedings of the Second International Conference on Case Histories in Geotechnical Engineering*, St. Louis, Mo., Paper No. 4.35, 1693-1701.

De Alba, P.A., Seed, H.B., Retamal, E., and Seed, R.B. 1988. Analysis of dam failures in 1985 Chilean earthquake. *Journal of Geotechnical Engineering*, ASCE, 114(12): 1414-1434.

Department of Water Resources 1989. Examination of the performance of Upper San Fernando Dam during the earthquake of February 9, 1971. *Addendum F of Bulletin 203-88 (The August 1, 1975, Oroville Earthquake Investigation, Supplement to Bulletin 203-78)*, The Resources Agency, State of California.

Fear, C.E. 1996. In-situ testing for liquefaction evaluation of sandy soils, *Ph.D. Thesis*, University of Alberta, Edmonton, Alberta, Canada.

Fear, C.E., and McRoberts, E.C. 1995. Reconsideration of initiation of liquefaction in sandy soils, Journal of Geotechnical Engineering, ASCE 121(3): 249-261.

Fear, C.E., and Robertson, P.K. 1995. Estimating the undrained shear strength of sand: a theoretical framework, Canadian Geotechnical Journal, 32(5): 859-870.

GEI Consultants 1988. Re-evaluation of the Lower San Fernando Dam, an investigation of the February 9, 1971 slide. *Submitted to U.S. Army Corps of Engineers, Waterways Experiment Station*, 2 Volumes.

Gu, W.H. 1992. Liquefaction and post-earthquake deformation analysis. *Ph.D. Thesis*, University of Alberta, Edmonton, Alberta, Canada.

Harder, L.F. 1988. Use of penetration tests to determine the cyclic loading resistance of gravelly soils during earthquake shaking. *Ph.D. Thesis*, Department of Civil Engineering, University of California, Berkeley.

Hazen, A. 1918. A study of the slip in the Calaveras Dam. *Engineering News-Record*, 81(26): 1158-1164.

Hazen, A. and Metcalf, L. 1918. Middle section of upstream side of Calaveras Dam slips into reservoir. *Engineering News-Record*, 80(14): 679-681.

Hryciw, R.D., Vitton, S., and Thomann, T.G. 1990. Liquefaction and flow failure during seismic exploration. *Journal of Geotechnical Engineering*, 116 (12): 1881-1899.

Ishihara, K. 1984. Post-earthquake failure of a tailings dam due to liquefaction of the pond deposit. *Proceedings of the International Conference on Case Histories in Geotechnical Engineering*, St. Louis, Mo, May 6-11, 3: 1129-1146.

Ishihara, K., and Koga, Y. 1981. Case studies of liquefaction in the 1964 Niigata earthquake, Soils and Foundations, 21(3): 35-52.

Jefferies, M.G., Been, K., and Hachey, J.E. 1990. Influence of scale on the constitutive behaviour of sand. *Proceedings of the 43rd Canadian Geotechnical Conference, Laval University*, 1: 263-273.

Konrad, J.-M., and Watts, B.D. 1995. Undrained shear strength for liquefaction flow failure analysis, Canadian Geotechnical Journal, 32(5): 783-794.

Lee, K.L., Seed, H.B., Idriss, I.M., and Makdisi, F.I. 1975. Properties of soil in the San Fernando hydraulic fill dams. *Journal of Geotechnical Engineering*, ASCE, 101(GT8): 801-821.

Little, T.E., Imrie, A.S., Psutka, J.F. 1994. Geologic and seismic setting pertinent to dam safety review of Duncan Dam. *Canadian Geotechnical Journal*, 31: 919-926.

Lucia, P.C. 1981. Review of experiences with flow failures of tailings dams and waste impoundments. *Ph.D. Thesis*, University of California, Berkeley.

Lucia, P.C., Duncan, J.M. and Seed, H.B. 1982. Summary of research on case histories of flow failures of mine tailings impoundments. *Proceedings of the Workshop on Mine Waste Disposal Technology*, Denver, Colorado, Bureau of Mines Information Circular 8857.

Marcusen, W.F. III, and Krinitzsky, E.L. 1976. Dynamic analysis of Fort Peck Dam. *Technical Report S-76-1*, U.S. Army Engineer Waterways Experiment Station, Vicksburg, Miss.

Marcusen, W.F. III, Ballard, R.F., Jr., and Ledbetter, R.H. 1979. Liquefaction failure of tailings dams resulting from the near Izu Oshima earthquake, 14 and 15 January, 1978. *Proceedings, 6th Pan-American Conference on Soil Mechanics and Foundations Engineering*, Lima, Peru.

McRoberts, E.C., and Sladen, J.A. 1992. Observations on static and cyclic sand liquefaction methodologies. *Canadian Geotechnical Journal*, 29, 4.

Middlebrooks, T.A. 1940. Fort Peck slide (with discussions by Messrs. J. Field, J.D. Justin, W. Gerig, A.J. Ryan, G. Gilboy, F.E. Fahlquist, I.B. Crosby and T.A. Middlebrooks). *ASCE Transactions*, Paper No. 2144, 723-764.

Mishima, S., and Kimura, H. 1970. Characteristics of landslides and embankment failures during the Tokachioki earthquake. *Soils and Foundations*, 10(2): 39-51.

NCEER 1998. Proceedings of the NCEER workshop on evaluation of liquefaction resistance of soils, Salt Lake City, Utah, January 1996, Edited by T.L. Youd and I.M. Idriss.

Pando, M., and Robertson, P.K. 1995. Evaluation of shear stress reversal due to earthquake loading for sloping ground, *Proceedings of the 48th Canadian Geotechnical Conference*, Vancouver, B.C., 2: 955-962.

Pillai, V.S., and Salgado, F.M. 1994. Post-liquefaction stability and deformation analysis of Duncan Dam. *Canadian Geotechnical Journal*, 31: 967-978.

Pillai, V.S., and Stewart, R.A. 1994. Evaluation of liquefaction potential of foundation soils at Duncan Dam. *Canadian Geotechnical Journal*, 31: 951-966.

Plewes, H.D., Pillai, V.S., Morgan, M.R., and Kilpatrick, B.L. 1994. In situ sampling, density measurements, and testing of foundation soils at Duncan Dam. *Canadian Geotechnical Journal*, 31: 927-938.

Popescu, R., Prevost, J.H., and Deodatis, G. 1997. Effects of spatial variability on soil liquefaction: some design recommendations, Geotechnique, 47(5): 1019-1036.

Poulos, S.J. 1988. Liquefaction and related phenomena. A*dvanced Dam Engineering for Design, Construction, and Rehabilitation*, R.B. Jansen (ed.), Van Nostrand Reinhold, New York, 292-320.

Robertson, P.K. 1994. Suggested terminology for liquefaction. Proceedings of the 47th Canadian Geotechnical Conference, Halifax, Nova Scotia, 277-286.

Robertson, P.K., and Fear, C.E. 1995. Liquefaction of sands and its evaluation. Keynote Lecture, Proceedings, IS Tokyo '95, 1st International Conference on Earthquake Geotechnical Eng., *Edited by* K. Ishihara, Balkema, Rotterdam, 3: 1253-1289.

Robertson, P.K., and Wride (née Fear), C.E. 1998. Cyclic liquefaction and its evaluation based on the SPT and CPT, Final submission to the 1996 NCEER Workshop on Evaluation of Liquefaction Resistance (T.L. Youd, Chair).

Rogers, B.T., Been, K., Hardy, M.D., Johnson, G.J., and Hachey, J. 1990. Re-analysis of Nerlerk B-67 berm failures. *Proceedings of the Canadian Geotechnical Engineering Conference*, Laval University, 1, 227-237.

Ross, G.A. 1968. Case studies of soil stability problems resulting from earthquakes. *Ph.D. Thesis*, University of California at Berkeley.

Ross, G.A., Seed, H.B., and Migliaccio, R.R. 1969. Bridge foundations in Alaska earthquake. *Journal of Soil Mechanics and Foundations Division*, ASCE, 95(4): 1007-1036.

Seed, H.B. 1969. Analysis of Sheffield Dam failure. *Journal of the Soil Mechanics and Foundations Division*, Proceedings of the ASCE, 95(SM 6): 1453-1490.

Seed, H.B. 1979. Considerations in the earthquake-resistant design of earth and rockfill dams. The Rankine Lecture, *Géotechnique*, 29(3): 215-263.

Seed, H.B. 1987. Design problems in soil liquefaction. *Journal of Geotechnical Engineering*, ASCE 113(8): 827-845.

Seed, R.B., and Harder, L.F. 1990. SPT-based analysis of cyclic pore pressure generation and undrained residual strength. *Proceedings of the H. Bolton Seed Memorial Symposium*, 2, 351-376.

Seed, H.B., Idriss, I.M., Lee, K.L., and Makdisi, F.I. 1975. Dynamic analysis of the slide in the lower San Fernando Dam during the earthquake of February 9, 1971. *Journal of the Geotechnical Engineering Division*, ASCE, 101(GT9): 889-912.

Seed, H.B, Tokimatsu, K., Harder, L.F., and Chung, R.M. 1984. The influence of SPT procedures in soil liquefaction resistance evaluations. *Earthquake Engineering Research Center Report No. UCB/EERC-84/15*, College of Engineering, University of California, Berkeley, California.

Seed, H.B., Seed, R.B., Harder, L.F., and Jong, H-L. 1988. Re-evaluation of the slide in the Lower San Fernando dam in the earthquake of Feb. 9, 1971. *Report No. UCB/EERC-88/04, Earthquake Engineering Research Center*, University of California, Berkeley.

Sego, D.C., Robertson, P.K., Sasitharan, S., Kilpatrick, B.L., and Pillai, V.S. 1994. Ground freezing and sampling of foundation soils at Duncan Dam. *Canadian Geotechnical Journal*, 31: 939-950.

Skempton, A. W. 1986. Standard penetration test procedures and the effects in sands of overburden pressure, relative density, particle size, ageing and overconsolidation. *Geotechnique*, 36(3): 425-447.

Sladen, J.A. 1989a. Cone penetration test calibration for Erksak (Beaufort Sea) sand: Discussion. *Canadian Geotechnical Journal*, 26: 173-177.

Sladen, J.A. 1989b. Problems with interpretation of sand state from cone penetration test. *Géotechnique*, 39(2): 323-332.

Sladen, J.A., and Hewitt, K.J. 1989. Influence of placement method on the in situ density of hydraulic sand fills. *Canadian Geotechnical Journal*, 26: 453-466.

Sladen, J.A., D'Hollander, R.D., Krahn, J. and Mitchell, D.E. 1985a. Back analysis of the Nerlerk berm liquefaction slides. *Canadian Geotechnical Journal*, 22: 579-588.

Sladen, J.A., D'Hollander, R.D., and Krahn, J. 1985b. The liquefaction of sands, a collapse surface approach. *Can. Geotech. J.*, 22: 564-578.

Sladen, J.A., D'Hollander, R.D., Krahn, J. and Mitchell, D.E. 1987. Back analysis of the Nerlerk berm liquefaction slides: Reply. *Canadian Geotechnical Journal*, 24: 179-185.

Stark, T.D., and Mesri, G.M. 1992. Undrained shear strength of liquefied sands for stability analysis. *Journal of Geotechnical Engineering*, ASCE, 118 (11): 1727-1747.

U.S. Army Corps of Engineers 1939. *Report on the slide of a portion of the upstream face of the Fort Peck Dam, Fort Peck, Montana.* U.S. Government Printing Office, Washington.

Yamada, G. 1966. Damage to earth structure and foundations by the Niigata earthquake June 16, 1964, in JNR. *Soils and Foundations*, 6(1): 1-13.

Yoshimine, M., Robertson, P.K., and Wride, C.E. Undrained shear strength of clean sands. Submitted to the Canadian Geotechnical Journal.

Youd, T. L. 1993. Liquefaction-induced lateral spread displacement. *Technical Note N-1862*, Naval Civil Engineering Laboratory, Port Hueneme, California.

Youd, T.L. and Bennett, M.J. 1983. Liquefaction sites, Imperial Valley, California. *Journal of Geotechnical Engineering*, ASCE, 109(3): 440-457.

Youd, T.L., Harp, E.L., Keefer, D.K., and Wilson, R.C. 1985. The Borah Peak, Idaho Earthquake of Oct. 28, 1983 -- liquefaction. *Earthquake Spectra*, Earthquake Engineering Research Institute, 2(1).

Table 1. Summary of the data by Seed and Harder (1990)

Case History No.	Name	S_u mean (psf)	S_u mean (kPa)	S_u +/- (psf)	S_u +/- (kPa)	$(N_1)_{60}$ in-situ	$(N_1)_{60}$ clean sand equivalent	FC (%)
1	Calaveras Dam	650	31.1	50	2.4	7	12	>60*
2	Sheffield Dam	75	3.6	25	1.2	4	6	25†
3	Fort Peck Dam	350	16.8	100	4.8	8	10	30*
4	Solfatara Canal Dike	50	2.4	25	1.2	4	4	<5*
5	Lake Merced Bank	100	4.8	0	0.0	6	6	3
6	Kawagishi-Cho Building	120	5.7	0	0.0	4	4	CS‡
7	Uetsu Railway Embankment	40	1.9	0	0.0	3	3	CS‡
8	Snow River Bridge Fill	50	2.4	0	0.0	5.5	7	15†
9	Koda Numa Embankment	50	2.4	0	0.0	3	3	CS‡
10	San Fernando Juvenile Hall	130	6.2	70	3.4	6	10.5	65
11	Lower San Fernando Dam	400	19.2	100	4.8	11.5	13.5	25
12	Upper San Fernando Dam	600	28.7	100	4.8	13	15	25
13a	Mochi-Koshi Tailings -Dam 2	250	12.0	150	7.2	0	5	80
13b	-Dam 1	--	--	--	--	--	--	--
14	Whiskey Springs Fan	150	7.2	10	0.5	8	11	40
15	La Marquesa Dam - U/S Slope	200	9.6	120	5.7	4	6	30
16	La Marquesa Dam - D/S Slope	400	19.2	150	7.2	9	11	20
17	La Palma Dam	200	9.6	100	4.8	3	4	15

* approximate values based on data from Poulos (1988); † estimated for this study; ‡ assumed to be clean sand (CS)

Note: In-situ values of $(N_1)_{60}$ were estimated from the clean sand equivalent values of $(N_1)_{60}$ using the following corrections, as proposed by Seed (1987): $\Delta(N_1)_{60}$ = 1, 2, 4 and 5 for FC = 10%, 25%, 50% and 75%, respectively

Table 2. Summary of case history statistics

Case History No.	Case History Name	Initial Slope Geometry Height* (m)	Initial Slope Geometry Angle† (°)	Type of Trigger	EQ Magnitude	a_{max} (in g)	Type of Failure	Post-failure Geometry Runout‡ (m)	Post-failure Geometry Angle (°)
1	Calaveras Dam	61	18.4	construction	N/A	N/A	flow	183	5.71
2	Sheffield Dam	7.6	21.8	EQ	6.3	0.15	flow	30	--
3	Fort Peck Dam	61	14	construction	N/A	N/A	flow	457	2.86
4	Solfatara Canal Dike	2.1	27	EQ	7.1	0.1 - 0.33	flow	23	3.6
5	Lake Merced Bank	9.8	34	EQ	5.7	0.12	slump	18	24
6	Kawagishi-Cho Building	0	0	EQ	7.5	--	building foundation	0	N/A
7	Uetsu Railway Embankment	10	29	EQ	7.5	--	flow	115	4
8	Snow River Bridge Fill	3	1.25	EQ	9.2	--	lateral spread	3	1.25
9	Koda Numa Embankment	3	30	EQ	8.1	--	flow	18	4
10	San Fernando Juvenile Hall	30	1.5	EQ	6.5	0.5	lateral spread	0.75	1.5
11	Lower San Fernando Dam	43	21.8	EQ	6.5	0.5 - 0.55	flow/slump	61	8.13
12	Upper San Fernando Dam	17.6	21.8	EQ	6.5	0.5 - 0.6	slump	1.5	21.8
13a	Mochi-Koshi Tailings -Dam 2	20	20.1	EQ	7	0.1 - 0.25	flow	240	4.5
13b	-Dam 1	30	20.1	EQ	7	0.1 - 0.25	flow	500	4.5
14	Whiskey Springs Fan	9.1	5	EQ	6.9	0.4	lateral spread	1.2	5
15	La Marquesa Dam - U/S Slope	7.9	27	EQ	8	0.6	slump	11	12.5
16	La Marquesa Dam - D/S Slope	7	34	EQ	8	0.6	slump	6.5	18
17	La Palma Dam	11	34	EQ	8	0.46	slump	5	17
18	Lake Ackerman	6.4	26.6	seismic explor.	N/A	CSR = 0.12	flow/slump	12	7.5
19	Nerlerk Embankment	24	12.65	construction	N/A	N/A	flow	100	1.5
20	Heber Road	0	0	EQ	6.55	>0.8	lateral spread	1.65	0
21	Duncan Dam	39	11.3	N/A	6.5	0.12	N/A	N/A	N/A

* The initial slope height was defined as the vertical distance from the toe to the crest of the pre-failure slope.

† If a slope was stepped, the initial slope angle represents most of the slope.

‡ Runout was defined as the horizontal distance from the toe of the original slope to the toe of the post-failure slope.

Notes: 1. Not enough information was given by Seed (1969) to estimate the post-failure slope angle for Sheffield Dam. 2. Details for Lake Merced Bank refer to Slide 1 reported by Ross (1968). 3. At San Fernando Juvenile Hall, there was a 30 m height difference between the toe and head of the slide since the lateral spread was 1.2 km long. 4. At Whiskey Springs Fan, there was a 9.1 m height difference between the toe and head of the slide since the lateral spread was 60 m long. 5. Details given for Nerlerk Embankment refer to the largest slide in 1983 (Slide 3). 6. At Heber Road, the ground was essentially level ground (i.e. slope angle $\approx 0°$); thus there was essentially no height difference between the toe and head of the spread area; horizontal displacements at Heber Road ranged from 4 ft to 7 ft at the road and canal, respectively; the average horizontal displacement was 5.5 ft (1.65 m). 7. The EQ data given for Duncan Dam are the design values.

Table 3. Additional key facts for each of the case histories

Case History No.	Case History Name	Year of Failure	No SPT Data	Reported as highly stratified deposit	Type of Structure	Direction of Failure	Nature of failure: Failed soil: large mass or distinct layer?	Nature of failure: Hinge-type motion observed	Nature of failure: Bearing capacity failure	Nature of failure: Reported as likely progressive	Nature of failure: Possibly associated with some weak shale or clay base layer
1	Calaveras Dam	1918	X		hydraulic fill dam	upstream	mass	X			
2	Sheffield Dam	1925	X		dam	downstream	layer beneath dam	X		X	
3	Fort Peck Dam	1938	limited		hydraulic fill dam	upstream	mass	X			X
4	Solfatara Canal Dike	1940	X		levee of a canal	away from canal	mass				
5	Lake Merced Bank	1957	X*		fill road embankment along lake	into lake	mass				
6	Kawagishi-Cho Building	1964	X‡		building on level ground	N/A	mass		X		
7	Uetsu Railway Embankment	1964	X		railway embankment	in one direction only	mass				
8	Snow River Bridge Fill	1964			bridges crossing river bed	downslope	mass				
9	Koda Numa Embankment	1968	X		highway embankment	in both directions	mass				
10	San Fernando Juvenile Hall	1971			gently sloping ground	downslope	layer				
11	Lower San Fernando Dam	1971	post-EQ D/S only	X	hydraulic fill dam	upstream	mass			X	
12	Upper San Fernando Dam	1971		X	hydraulic fill dam	downstream (limited)	mass				
13a	Mochi-Koshi Tailings -Dam 2	1978			tailings dam	downstream	mass			X	
13b	-Dam 1	1978			tailings dam	downstream	mass				
14	Whiskey Springs Fan	1983	BPT data only		gently sloping ground	downslope	mass				
15	La Marquesa Dam - U/S Slope	1985			storage reservoir dam	upstream	layer beneath dam				
16	La Marquesa Dam - D/S Slope	1985			storage reservoir dam	downstream	layer beneath dam				
17	La Palma Dam	1985			storage reservoir dam	upstream	layer beneath dam				
18	Lake Ackerman	1987			hydraulic fill road embankment	into lake	layer				
19	Nerlerk Embankment	1983	CPT data only		subsea hydraulic fill berm	various directions	mass			X	X
20	Heber Road	1979			gently sloping ground	downslope	layer				
21	Duncan Dam	N/A			zoned earthfill hydroelectric dam which is founded on sandy soil	no failure	N/A				

Notes: References†: 1. Hazen and Metcalf (1918), Hazen (1918); 2. Seed (1969); 3. US Army Corps of Eng. (1939), Casagrande (1965), Middlebrooks (1940), Marcusen & Krinitzsky (1976); 4. Ross (1968); 5. Ross (1968); 6. Yamada (1966)‡; 7. Yamada (1966), Lucia (1981), Lucia et al. (1982); 8. Ross et al. (1969; 9. Mishima & Kimura (1970), Lucia (1981), Lucia et al. (1982); 10. Bennett (1989); 11. Seed et al. (1975), Seed (1979), Davis et al. (1988), Seed et al. (1988), McRoberts & Sladen (1992), Gu (1992); 12. Lee et al. (1985), Dept. of Water Resources (1989); 13a&b. Marcusen et al. (1979), Ishihara (1984), Baziar & Dobry (1995); 14. Harder (1988), Youd et al. (1985), Andrus et al. (1986), Andrus & Youd (1987), Andrus & Youd (1989); 15, 16 & 17. De Alba et al. (1988); 18. Hryciw et al. (1990); 19. Sladen et al. (1985a), 1987), Rogers et al. (1990), Sladen & Hewitt (1989), Been et al. (1986, 1987a,1987b); 20. Davis et al. (1988), Youd & Bennett (1983); 21. Little et al. (1994), Sego et al. (1994), Plewes et al. (1994), Pillai & Stewart (1994), Pillai & Salgado (1994), Byrne et al. (1994).

* The SPT data were from two boreholes through natural soil; however, the failure appears to be due to failure of the underwater fill in which no SPT data are available

† In addition to the three main references: Seed (1987), Seed and Harder (1990), Stark and Mesri (1992)

‡ Yamada (1966) did not specifically discuss the Kawagishi-Cho Building; however, it did refer to the Niigata Railway Station which was founded on piles and did not fail during the EQ and mentioned that "neighboring buildings without pile foundation[s] suffered severe unequal settlement or tipping"

Table 4. $(N_1)_{60}$ values selected by various authors for each of the case histories

Case History No.	Name	Researchers	$(N_1)_{60}$ In-situ	$(N_1)_{60}$ Clean sand equivalent	FC (%)	Comments
1	Calaveras Dam	Seed (1987)		12		Typical value for hydraulic sand fill in original structure, based on "tests performed in recent years"
	* No SPTs performed	Seed & Harder (1990)		12		Adopted value by Seed (1987)
		Stark & Mesri (1992)		12		Adopted value by Seed (1987)
		Poulos (1988)		7	> 60	Adopted N_1=2; assuming ER=60% & FC>60%, gives $(N_1)_{60}$-cs = 7
2	Sheffield Dam	Seed (1969)				Estimated D_r of 35 to 40% for upper 1 to 1.5 feet of foundation material, based on degree of compaction of about 76%
	* No SPTs performed	Seed (1987)		6 to 8		Based on estimated D_r of 40 to 50%; appears to use correlations such as in Skempton (1986)
		Seed & Harder (1990)		6		
		Stark & Mesri (1992)		6		
3	Fort Peck Dam	Marcusen & Krinitzsky (1976)	≥ 7			D_r of 40 to 50% in shell material and 55% in foundation sands
	* Limited SPTs performed	Seed (1987)		11 to 12		Based on foundation sands having a D_r of 45 to 50%, based on Marcusen & Krinitzsky (1976)
		Poulos (1988)		7.3	30	Adopted N_1=5.3; assuming ER=60% & FC=30%, gives $(N_1)_{60}$-cs =7.3
4	Solfatara Canal Dike	Ross (1968)				Noted that original north levee could be considered to have had a similar D_r to the existing south levee, which was estimated from borings to be about 32%
	* No SPTs performed	Seed (1987)		5		Based on a relative density of 30% and the fact that the sand is clean uniform fine sand
		Poulos (1988)		0	<5	Adopted N_1=0 ($D_r \approx 32\%$); assuming ER=60% & FC<5%, gives $(N_1)_{60}$-cs = 0
5	Lake Merced Bank	Ross (1968)				Range in raw N (based on BH1 and BH2 combined): 4 to 21 (average 11) in unit B, 8 to 24 (average 16) in unit C
		Seed (1987)		5		Estimated D_r of 40%
		Seed & Harder (1990)		6		
		Stark & Mesri (1992)		6	3	
		This study	7**			Two boreholes: BH1 (located outside failure zone); BH2 (located within slide area). Unit B average raw N is 4 to 21 (avg. 16) in BH1 and 4 to 10 (avg. 7) in BH2; BH2 results in $(N_1)_{60}$ in-situ = 7. ** However, BH1 was located well outside fill, through natural soil; BH2 was located on the outside edge of the cut/fill boundary of the highway, through natural soils. It appears that the soil that played the predominant role in the failure was underwater fill. SPT results in natural soil have no meaning for the fill; therefore, remove case history from the database.
6	Kawagishi-Cho Building	Seed (1987)				not less than 4 (referring to paper by Yamada, 1966)
	* SPTs reported by Yamada (1966) were performed at a nearby building only	This study				A value of 4 is probably reasonable: low blowcounts of raw N = 2 to 4.5 were recorded in the upper sand layer beneath the Railway Station (Yamada, 1966); it appears that the ground conditions beneath the Kawagishi-Cho building were assumed to be similar (probably a good assumption, based on an SPT sounding for Kawagishi-Cho site presented by Ishihara & Koga, 1981)
7	Uetsu Railway Embankment	Seed (1987)		< 3		"since the embankment had performed satisfactorily under train loadings before the earthquake, it [was] unlikely that the [equivalent clean sand] $(N_1)_{60}$ value for the sand was less than about 3"
	* No SPTs performed	Seed & Harder (1990)		3		
		Stark & Mesri (1992)		3		
8	Snow River Bridge Fill	Ross et al. (1969)				Raw N of 5 to 10 in upper 40 to 50 ft of river bed and increasing to 30 at tips of deepest piles (≈ 60 feet)
		Seed (1987)		7		Value given in Seed (1987) text (Noted that the soil involved in the lateral slide was a gravelly sand)
				5		Value given in Seed (1987) table
		Seed & Harder (1990)		7		
		Stark & Mesri (1992)	5	7 to 10	10 to 30	
9	Koda Numa Embankment	Seed (1987)		3 to 4		Seed (1987) felt that the $(N_1)_{60}$-cs "is not likely to be less than about 3 or 4 in a railway embankment of this type" since the embankment had performed satisfactorily under loadings prior to the earthquake, similar to the Uetsu Railway Embankment
	* No SPTs performed	Seed & Harder (1990)		3		
		Stark & Mesri (1992)		3		
10	San Fernando Juvenile Hall	Seed (1987)	2	6		For the saturated sandy silt in unit B1
		Davis et al. (1988)	4		50 to 75	
		Bennett (1989)	3.7 to 11.2			Average value = 7.9
		Seed & Harder (1990)	6*	10	65	* Note: it appears that the value of $(N_1)_{60}$-cs reported by Seed & Harder (1990) has been double corrected for fines content since the value they assumed as the in-situ $(N_1)_{60}$ was 6; however, this was the equivalent clean sand value reported by Seed (1987), having already been corrected for fines content from the in-situ $(N_1)_{60}$ of 2
		Stark & Mesri (1992)	6*	10.5 to 13.0	65	* Note: same comment as for Seed & Harder (1990) $(N_1)_{60}$-cs value

11 Lower San Fernando Dam	Seed (1987)				Based on a post-EQ average $(N_1)_{60}$ in D/S shell of about 16 and D_r of about 50 to 55%; assumed pre-EQ values would be lower; selected $(N_1)_{60}$cs of 15 based on D_r of 50%
* Post-EQ SPTs in downstream shell only	Seed et al. (1988)	11.5	13.5	25 to 30	Pre-EQ $(N_1)_{60}$ in-situ in U/S shell estimated from average $(N_1)_{60}$ in-situ of 14.5 in D/S shell (post-EQ), corrected to 12.5 downstream (pre-EQ), corrected to 11.5 upstream (pre-EQ) Final correction to $(N_1)_{60}$cs of 13.5 based on FC of 25 to 30%
	Poulos (1988)			50	Adopted N_1=8.5; assuming ER=60% and FC=50%; no indication as to if this was for U/S or D/S side
	Davis et al. (1988)	5.5*	7.5 to 9.5*	50	Assigned an $(N_1)_{60}$ of 8.5 to the downstream side of the dam * Note: if $(N_1)_{60}$ of 8.5 is assumed to be the in-situ $(N_1)_{60}$ in the D/S site, it becomes an U/S, pre-EQ $(N_1)_{60}$ in situ of 5.5, using the $\Delta(N_1)_{60}$ values applied by Seed et al. (1988); this converts to an $(N_1)_{60}$-cs of 9.5 for FC = 50%; however, for FC = 25 to 30% (like Seed et al., 1988, assumed), $(N_1)_{60}$cs = 7.5
	Seed & Harder (1990)	11.5	13.5		
	Stark & Mesri (1992)	11.5	13.5 to 17.5	25 to 30	Clean sand equivalent value depends on type of correction factor used
	McRoberts & Sladen (1992)		7		Based on a sensible lower bound for the post-EQ D/S in-situ $(N_1)_{60}$ of 8, converted to a pre-EQ U/S $(N_1)_{60}$-cs of 7
			4		Based on CPT logs from 1985 fieldwork (GEI Consultants, 1988), giving a lower bound post-EQ D/S tip resistance of 24 bars (25 tsf) and converting to a post-EQ D/S $(N_1)_{60}$cs of 7 or a pre-EQ U/S $(N_1)_{60}$-cs of 4
12 Upper San Fernando Dam	Dept. of Water Resources (1989)	13	15	25	Based on average post-earthquake $(N_1)_{60}$ in-situ of 17.5 in lower elevations of the hydraulic fill, corrected to pre-earthquake average $(N_1)_{60}$ of 13, corrected to pre-earthquake average $(N_1)_{60}$cs of 15 for FC = 25% (N.B. correction from post-earthquake to pre-earthquake of 4.5 blows based on estimated relative density change of 12%)
	Seed & Harder (1990)	13	15	25	
	Stark & Mesri (1992)	13	15 to 19	25	Clean sand equivalent value depends on type of correction factor used
13 Mochi-Koshi Tailings 13a – Dam 2	Ishihara (1984)			85	In tailings pond, raw N of 0 down to 15 m, at which raw N = 3 to 7; in starter dikes (did not fail), raw N about 5
	Seed (1987)	1	6		
	Poulos (1988)	0		> 60	
	Davis et al. (1988)	0		> 60	
	Seed & Harder (1990)	0	5	80	
	Stark & Mesri (1992)	0	5 to 7	80	Clean sand equivalent value depends on type of correction factor used
13b- Dam 1	This study	0	5		Assumed same values as for Dam 2 (Seed & Harder, 1990)
14 Whiskey Springs Fan	Harder (1988)	8	10	20	Based on Becker Penetration Test (BPT) values converted to equivalent SPT values; total fines content = 20%
* No SPTs performed; BPTs were converted to SPT values	Seed & Harder (1990)	8	11	40	40% FC based on sand matrix alone
	Stark & Mesri (1992)	8	11 to 15	40	Clean sand equivalent value depends on type of correction factor used
	Andrus & Youd (1989)	6 to 12			Average CPT results converted to equivalent SPT values
15 La Marquesa Dam - U/S Slope	De Alba et al. (1988)	4*	6	30	* Note, however, that only two blowcounts were measured in the silty sand layer that liquefied
	Seed & Harder (1990)	4	6		
	Stark & Mesri (1992)	4	6 to 10		Clean sand equivalent value depends on type of correction factor used
16 La Marquesa Dam - D/S Slope	De Alba et al. (1988)	9*	11	20	* Only three blowcounts in layer that liquefied; 9 = highest value
	Seed & Harder (1990)	9	11		
	Stark & Mesri (1992)	9	11 to 14		Clean sand equivalent value depends on type of correction factor used
	This study	5.5	7.5	20	Lower bound approach
17 La Palma Dam	De Alba et al. (1988)	3	4	15	* In the damaged area, the only blowcounts measured in the loose silty sand layer were one blowcount in each of two boreholes located midslope.
	Seed & Harder (1990)	3	4		
	Stark & Mesri (1992)	3	4 to 7	15	Clean sand equivalent value depends on type of correction factor used
18 Lake Ackerman	Hryciw et al. (1990)	3			$(N_1)_{60}$ in-situ: 6 to 8 (failed section); 1 to 4 in (unfailed section)
	Stark & Mesri (1992)	3	4	0 to 5	
19 Nerlerk Embankment * No SPTs performed	Jefferies et al. (1990)		11		Inferred from CPT results
	Stark & Mesri (1992)	10 to 11	10 to 12.5	0 to 10	Referred to Jefferies et al. (1990); Clean sand equivalent value depends on type of correction factor used
20 Heber Road	Youd & Bennett (1983)				Raw N of 1 to 7 (safety hammer) or 2 to 4 (donut hammer)
	Davis et al. (1988)	1.4		15	Based on raw N of 1 over a depth of 6 to 11 feet
	Stark & Mesri (1992)	1	1.5 to 5	15	Clean sand equivalent value obtained depends on type of correction factor used
21 Duncan Dam	Plewes et al. (1994) and Pillai & Stewart (1994)	10 to 18.5			$(N_1)_{60}$ values increased with depth in soil unit of interest (see Table 5)

Table 5. S_u values selected by various authors for each of the case histories

Case History No.	Name	Researchers	S_u (psf)	Comments
1	Calaveras Dam	Seed (1987)	750	Based on post-failure configuration of slide mass; no specific details are given
		Poulos (1988)	700	Incorporated effects of energy and dynamics of failure; calculated 1500 psf for pre-failure driving stress, 250 psf for post-failure driving stress, and 600 psf to 1100 psf for mobilized undrained shear strength; 700 psf is recommended value
		Davis et al. (1988)	700	Same results as Poulos (1988)
		Seed and Harder (1990)	650 ± 50	No explanation given; appears to represent range from the minimum value of 600 psf to recommended value of 700 psf, given by Poulos (1988)
		Stark and Mesri (1990)	650 ± 50	
2	Sheffield Dam	Seed (1987)	50	Based on a simple calculation assuming the entire base liquefied and acted as slip surface with thrust leading to failure a result of the 15 ft deep upstream reservoir
		Seed and Harder	75 ± 25	No explanation
		Stark and Mesri	76 ± 25	No explanation
3	Fort Peck Dam	Lucia (1981), Lucia et al. (1982)	250	Based on post-failure configuration of the slide mass
		Seed (1987)	600	No specific explanations; stated that "other studies indicate a pre-sliding driving stress of about 700 psf; a reasonably conservative value [for S_u] is 600 psf"
		Poulos (1988)	700	Incorporated effects of energy and dynamics of failure; calculated 1800 psf for pre-failure driving stress, 50 psf for post-failure driving stress, and 500 psf to 1100 psf for mobilized undrained shear strength; 700 psf is recommended value
		Davis et al. (1988)	700	
		Seed & Harder (1990)	350 ± 100	
		Stark & Mesri (1992)	351 ± 100	
4	Solfatara Canal Dike	Seed (1987)	130	"the average shear stress at the base of the dike"; no further details given
		Poulos (1988)		Incorporated effects of energy and dynamics of failure; calculated 105 psf for pre-failure driving stress, 0 psf for post-failure driving stress; no specific value was calculated for the mobilized undrained shear strength, but concluded it would have to be greater than 0 psf
		Seed & Harder (1990)	50 ± 25	No explanation
		Stark & Mesri (1992)	51 ± 25	No explanation
5	Lake Merced Bank	Seed (1987)	100	No explanation
		Seed & Harder (1990)	100	
		Stark & Mesri (1992)	100	
6	Kawagishi-Cho Building	Seed (1987)	120	Value calculated as the average shear stress in the foundation, based on an estimated average base pressure from the building of 600 psf; thus, it appears that S_u was calculated using the plasticity theory undrained foundation failure equation of $q_f = 5.14\ S_u$, where q_f is the base pressure from the building
		Seed & Harder (1990)	120	
		Stark & Mesri (1992)	120	
7	Uetsu Railway Embankment	Lucia (1981), Lucia et al. (1982)	35	Based on post-failure configuration of the slide mass
		Seed (1987)	35	Adopted the value from the work of Lucia (1981), Lucia et al. (1982)
		Seed & Harder (1990)	40	No explanation
		Stark & Mesri (1992)	40	
		This study	37.5 ± 2.5	Based on reported range of 35 to 40 psf; however, value would be larger if energy effects had been taken into account, as done by Poulos (1988) and Davis et al. (1988) for some of the case histories
8	Snow River Bridge Fill	Seed (1987)	50	Concluded that "the residual strength of the liquefied sand was very low, probably about 50 psf, for movements of about 10 ft to have occurred"; no other explanation given, but possibly something like a Newmark sliding block analysis was used
		Seed & Harder (1990)	50	
		Stark & Mesri (1992)	50	
9	Koda Numa Embankment	Lucia (1981), Lucia et al. (1982)	25	Based on post-failure configuration of slide mass which flowed over level ground
		Seed (1987)	25	Value in Seed (1987) text (referring to the work by Lucia (1981), Lucia et al. (1982))
			50	Value in Seed (1987) table
		Seed & Harder (1990)	50	
		Stark & Mesri (1992)	50	
10	San Fernando Juvenile Hall	Seed (1987)	140	Newmark-type deformation analysis for a maximum ground surface acceleration of 0.6g and the 5 ft observed surface displacements
		Davis et al. (1988)	200	Incorporated effects of energy and dynamics of failure, using a Newmark-type analysis; calculated 55 psf for both the pre- and post-failure driving stresses and a mobilized undrained shear strength of 50 to 450 psf with recommendation to use an S_u of 200 psf
		Seed & Harder (1990)	130 ± 70	No explanation given; upper end coincides with recommendation by Davis et al. (1988)
		Stark & Mesri (1992)	131 ± 70	
11	Lower San Fernando Dam	Seed (1987)	750	Estimated based on the pre-failure slope configuration and assigning know strengths to the non-liquefied zones at the toe and crest of the slope
		Seed et al. (1988)	580	35-percentile strength of 850 psf (the pre-EQ U/S S_u estimated by steady-state analysis) (N.B. reported that "actual residual shear strength determined from configuration when slide mass stopped moving" was 400 ± 100 psf; lower bound of this range calculated "knowing that sliding would stop when the factor of safety attained a value of unity" and "based on the configuration of the slide mass at the end of sliding"; upper bound calculated by allowing for "the inertia effects associated with the rate of movement and a possible 70% reduction in strength of the liquefied soil as it moves into the reservoir")

		Davis et al. (1988)		Incorporated effects of energy and dynamics of failure; calculated 950 psf for pre-failure driving stress and 510 psf for mobilized undrained shear strength
		Poulos (1988)	750	Incorporated effects of energy and dynamics of failure; calculated 1000 psf for pre-failure driving stress, and 500 to 1000 psf for mobilized undrained shear strength; 750 psf is recommended value
		Seed & Harder (1990)	400 ± 100	Based on findings of Seed et al. (1988)
		Stark & Mesri (1992)	401 ± 100	
		Gu (1992)		Finite element post-earthquake deformation analyses, based on collapse mechanics and ultimate state strengths, investigating stress redistribution; found that the observed progressive failure wold be predicted if the ultimate state strength in the hydraulic fill were lower than the average value based on laboratory tests reported by Seed et al. (1988)
12	Upper San Fernando Dam	Dept. of Water Resources (1989)	500 to 700	Liquefied zone (Zone IV) predicted to have occurred in bottom half of hydraulic fill, based on earthquake-induced compressive strain potential analysis; S_u values calculated based on FS=1 for a circular failure surface through the pre-failure dam configuration and assuming strength parameters for the other, non-liquefied zones (range in S_u values based on range in strength parameters assigned to the partially liquefied zone around Zone IV)
		Seed & Harder (1990)	600 ± 100	
		Stark & Mesri (1992)	601 ± 100	
13	Mochi-Koshi Tailings 13a - Dam 2	Lucia (1981), Lucia et al. (1982)	210	Based on post-failure configuration of the tailings remaining in the tailings pond
		Seed (1987)	210	Value in Seed (1987) test (Referred to work by Lucia (1981), Lucia et al. (1982))
			250	Value in Seed (1987) table
		Poulos (1988)		Incorporated effects of energy and dynamics of failure; calculated 390 psf for pre-failure driving stress, 100 psf for post-failure driving stress, and 75 to 200 psf for mobilized undrained shear strength; 130 psf is recommended value
		Davis et al. (1988)	250	
		Seed & Harder (1990)	250 ± 150	
		Stark & Mesri (1992)	250 ± 150	
	13b - Dam 1	Poulos (1988)	60	Incorporated effects of and dynamics of failure; calculated 540 psf for pre-failure driving stress, < 50 psf for post-failure driving stress, and 50 to 110 psf for mobilized undrained shear strength; 60 psf is recommended value
		Davis et al. (1988)	60	
14	Whiskey Springs Fan	Harder (1988)	130 to 160	Lower bound estimated using a stability analysis under static loading conditions and determining S_u for FS=1; upper bound estimated using 1978 Makdisi-Seed modification of Newmark's sliding block double integration method, based on 1.2 m of movement
		Seed & Harder (1990)	150 ± 10	Referred to Harder (1988), but used a slightly narrower range
		Stark & Mesri (1992)	150 ± 10	
15	La Marquesa Dam - U/S Slope	De Alba et al. (1988)	76 to 340	Lower bound estimated based on the post-failure configuration and equals the post-failure driving stress; upper bound based on the initial configuration of the slope, including horizontal stresses from the core plus inertia effects
		Seed & Harder (1990)	200 ± 120	
		Stark & Mesri (1992)	200 ± 120	
16	La Marquesa Dam - D/S Slope	De Alba et al. (1988)	266 to 580	Lower bound estimated based on the post-failure configuration and equals the post-failure driving stress; upper bound based on the initial configuration of the slope, including horizontal stresses from the core plus inertia effects
		Seed & Harder (1990)	400 ± 150	
		Stark & Mesri (1992)	400 ± 150	
17	La Palma Dam	De Alba et al. (1988)	120 to 300	Lower bound estimated based on the post-failure configuration and equals the post-failure driving stress. Upper bound based on the initial configuration of the slope, including horizontal stresses from the core plus inertia effects
		Seed & Harder (1990)	200 ± 100	
		Stark & Mesri (1992)	200 ± 100	
18	Lake Ackerman	Hryciw et al. (1990)	170 to 260	Both strengths estimated using 2-D stability analyses, one in failed zone (giving S_u= 260 psf) and one in the zone that did not fail, although seismic trucks had passed over it (giving S_u = 170 psf); analysis assumed a single S_u throughout both the loose sand fill and the denser sand above the groundwater table; therefore, S_u may be overpredicted
19	Nerlerk Embankment	Sladen et al. (1985a)	< 42 psf	For all slides in Nerlerk embankment; represents steady state strength required for limiting equilibrium of an infinite slope, based on the ranges in post-failure slope angles and thicknesses of the failed soil masses (did not take into account dynamics of the failure, as done by Poulos (1988) and Davis et al. (1988) for other cases)
		Jefferies et al. (1990)		S_u/σ'_{vo} = approximately 0.15 (K_o = 0.7)
		Stark & Mesri (1992)		S_u/σ'_{vo} = 0.148, based on Jefferies et al. (1990); based on average embankment height of 12 m and estimated unit weight of soil of about 18 kN/m^3, this strength ratio translates into an average S_u of approximately 14.4 kPa (300 psf)
20	Heber Road	Davis et al. (1988)	100 psf	Incorporated effects of energy and the dynamics of the lateral spread, using a Newmark type analysis to match observed movements; results indicated both pre- and post-failure driving stresses of 40 psf and mobilized S_u of 100 psf
		Stark & Mesri (1992)	100 psf	
21	Duncan Dam	Pillai & Salgado (1994)		S_u/σ'_{vo} = 0.21, based on laboratory testing on undisturbed frozen samples (based on post-cyclic undrained monotonic simple shear test results)

Table 6. Duncan Dam results (Byrne et al., 1994)

σ_v' (kPa)	σ_v' (psf)	$S_u=0.21\sigma_v'$ (kPa)	S_u (psf)	$(N_1)_{60}$ in-situ
100	2089	21	439	10
200	4177	42	877	11
300	6266	63	1316	12.4
400	8354	84	1754	13.2
600	12531	126	2632	14.5
800	16708	168	3509	15.7
1000	20886	210	4386	17.3
1200	25063	252	5263	18.5

Note: $S_u = 0.21\sigma'_v$ is based on undrained monotonic direct simple shear testing of undisturbed samples

Table 7. Summary of deformation analysis

Case History No.	Name	Runout Height (m/m)	Horizontal Strain (%)	Post angle Pre angle	Brittleness Index $I_B = \frac{\tan\beta_i - \tan\beta_f}{\tan\beta_i}$	σ'_{vi} (Stark & Mesri, 1992) (psf)	σ'_{vi} (Stark & Mesri, 1992) (kPa)	Approx. RSR (p'_i/p'_{us})
1	Calaveras Dam	3.0	99.8	0.31	0.70	2855	136.7	1.8
2	Sheffield Dam	3.9	157.9			1975	94.6	10.5
3	Fort Peck Dam	7.5	186.8	0.20	0.80	10815	517.8	12.4
4	Solfatara Canal Dike	11.0	558.1	0.13	0.88	955	45.7	7.6
5	Lake Merced Bank	1.8	123.9	0.71	0.34	950	45.5	3.8
6	Kawagishi-Cho Building					1225	58.7	4.1
7	Uetsu Railway Embankment	11.5	637.5	0.14	0.87	2690	128.8	26.9
8	Snow River Bridge Fill	1.0	2.2	1.00	0.00	2100	100.5	16.8
9	Koda Numa Embankment	6.0	346.4	0.13	0.88	1550	74.2	12.4
10	San Fernando Juvenile Hall	0.0	0.1	1.00	0.00	1940	92.9	6.0
11	Lower San Fernando Dam	1.4	56.7	0.37	0.64	3930	188.2	3.9
12	Upper San Fernando Dam	0.1	3.4	1.00	0.00	2975	142.4	2.0
13a	Mochi-Koshi Tailings -Dam 2	12.0	439.1	0.22	0.78	2715	130.0	4.3
13b	-Dam 1	16.7	609.9	0.22	0.78	4072.5	195.0	
14	Whiskey Springs Fan	0.1	1.2	1.00	0.00	2630	125.9	7.0
15	La Marquesa Dam - U/S Slope	1.4	70.9	0.46	0.56	1600	76.6	3.2
16	La Marquesa Dam - D/S Slope	0.9	62.6	0.53	0.52	1790	85.7	1.8
17	La Palma Dam	0.5	30.7	0.50	0.55	1670	80.0	3.3
18	Lake Ackerman	1.9	93.9	0.28	0.74	1845	88.3	--
19	Nerlerk Embankment	4.2	93.5	0.12	0.88	--	--	--
20	Heber Road	--	--	--	--	800	38.3	--
21	Duncan Dam	N/A	N/A	N/A	N/A	--	--	--

Note: Horizontal strain = observed runout divided by initial slope length, where initial slope length = horizontal distance from the toe of the initial slope to the point immediately below the crest of the initial slope (i.e. calculated from initial slope height and angle).

Table 8. Summary of range in data reported by various authors

Case History No.	Name	S_u Minimum (psf)	S_u Minimum (kPa)	S_u Maximum (psf)	S_u Maximum (kPa)	S_u Avg. of Max/Min (psf)	S_u Avg. of Max/Min (kPa)	S_u +/- for Max/Min (psf)	S_u +/- for Max/Min (kPa)	$(N_1)_{60}$ in-situ Minimum	$(N_1)_{60}$ in-situ Maximum	$(N_1)_{60}$ in-situ Avg. of Max/Min	$(N_1)_{60}$ in-situ +/- for Max/Min	FC Minimum (%)	FC Maximum (%)
1	Calaveras Dam	600	28.7	750	35.9	675	32.3	75	3.6	2	7	4.5	2.5		>60
2	Sheffield Dam	50	2.4	100	4.8	75	3.6	25	1.2	4	6	5	1		25*
3	Fort Peck Dam	250	12.0	700	33.5	475	22.7	225	10.8	5.3	10	7.65	2.35		30
4	Solfatara Canal Dike	0	0.0	130	6.2	65	3.1	65	3.1	0	4	2	2		<5
5	Lake Merced Bank	100	4.8	100	4.8	100	4.8	0	0.0	5	7	6	1	3	3
6	Kawagishi-Cho Building	120	5.7	120	5.7	120	5.7	0	0.0	4	4	4	0		
7	Uetsu Railway Embankment	35	1.7	40	1.9	38	1.8	3	0.1	3	3	3	0		
8	Snow River Bridge Fill	50	2.4	50	2.4	50	2.4	0	0.0	5	5.5	5.25	0.25		
9	Koda Numa Embankment	25	1.2	50	2.4	38	1.8	13	0.6	3	4	3.5	0.5		
10	San Fernando Juvenile Hall	60	2.9	200	9.6	130	6.2	70	3.4	2	6	4	2	50	65
11	Lower San Fernando Dam	300	14.4	750	35.9	525	25.1	225	10.8	5.5	11.5	8.5	3	25	25
12	Upper San Fernando Dam	500	23.9	700	33.5	600	28.7	100	4.8	13	13	13	0	25	>60
13a	Mochi-Koshi Tailings -Dam 2	100	4.8	400	19.2	250	12.0	150	7.2	0	1	0.5	0.5	>60	80
13b	-Dam 1	50	0.0	110	0.0	80	3.8	30	1.4	0	1	0.5	0.5	>60	80
14	Whiskey Springs Fan	130	6.2	160	7.7	145	6.9	15	0.7	6	12	9	3	40	40
15	La Marquesa Dam - U/S Slope	76	3.6	340	16.3	208	10.0	132	6.3	4	4	4	0	30	30
16	La Marquesa Dam - D/S Slope	266	12.7	580	27.8	423	20.3	157	7.5	9	9	9	0	20	20
17	La Palma Dam	100	4.8	300	14.4	200	9.6	100	4.8	3	3	3	0	15	15
18	Lake Ackerman	170	8.1	260	12.4	215	10.3	45	2.2	3	3	3	0	0	5
19	Nerlerk Embankment	42	2.0	300	14.4	171	8.2	129	6.2	10	11	10.5	0.5	2	12
20	Heber Road	100	4.8	100	4.8	100	4.8	0	0.0	1	1	1	0		29

* estimated for this study

Table 9. Summary of minimum $(N_1)_{60}$ approach

Case History No.	Name	Type of Failure	S_u mean (psf)	S_u mean (kPa)	$(N_1)_{60}$ in-situ	$(N_1)_{60}$ clean sand equivalent	FC (%)	Comments
1	Calaveras Dam	flow	700	33.5	2	7	>60	Minimum N_1 and S_u from Poulos (1988); assumed $N_1=(N_1)_{60}$ (i.e. ER=60%)
2	Sheffield Dam	flow	75	3.6	4	6	25†	Used lowest stated D_r=35% and $(N_1)_{60}/D_r^2$=48 for clean sand equivalent and =34 for in-situ
3	Fort Peck Dam	flow	700	33.5	5	7	30	S_u from Davis et al. (1988); N_1 from Poulos (1988); assumed $N_1=(N_1)_{60}$ (i.e. ER=60%)
4	Solfatara Canal Dike	flow	50	2.4	0	0	<5	N_1 from Poulos (1988); assumed $N_1=(N_1)_{60}$ (i.e. ER=60%)
5	Lake Merced Bank	slump	100	4.8	5	5	3	Case record validity doubtful; no data from fill in lake; data from natural ground behind failure zone
6	Kawagishi-Cho Building	building foundation	120	5.7	4	4	CS‡	Case record is different from all other cases because it was not a slope
7	Uetsu Railway Embankment	flow	80	3.8	3	3	CS‡	Original S_u based on runout; doubled to account for energy effects
8	Snow River Bridge Fill	lateral spread	50	2.4	5	6.5	15†	
9	Koda Numa Embankment	flow	50	2.4	3	3	CS‡	
10	San Fernando Juvenile Hall	lateral spread	200	9.6	2	6	65	S_u from Davis et al. (1988); original Seed (1987) $(N_1)_{60}$=2; Seed & Harder (1990) applied ΔN twice
11	Lower San Fernando Dam	flow/slump	500	23.9	6	8	25	$(N_1)_{60}$ from lower bound assessment of sandy SPTs in GEI (1988) and S_u from Davis et al. (1988)
12	Upper San Fernando Dam	slump	600	28.7	5.5	7.5	25	Department of Water Resources (1989) Figure 432 data corrected to pre-event
13a	Mochi-Koshi Tailings -Dam 2	flow	130	6.2	0	5	80	S_u from Davis et al. (1988) and Poulos (1988); $(N_1)_{60}$ from Ishihara (1984)
13b	-Dam 1	flow	60	0.0	0	5	80	As above
14	Whiskey Springs Fan	lateral spread	150	7.2	5	8	40	$(N_1)_{60}$ from Andrus and Youd (1989) from Becker equivalents
15	La Marquesa Dam - U/S Slope	slump	200	9.6	4	6	30	
16	La Marquesa Dam - D/S Slope	slump	400	19.2	5.5	7.5	20	
17	La Palma Dam	slump	200	9.6	3	4	15	
18	Lake Ackerman	flow/slump	215	10.3	3	3	0	
19	Nerlerk Embankment	flow	315	15.1	3	4	10	Lower bound $(N_1)_{60}$ based on Sladen et al. (1985) CPT data and $q_{c1}/(N_1)_{60}$=0.5
20	Heber Road	lateral spread	100	4.8	1	3	29	Spread for soil A2 also in Seed et al. (1985) trigger database; see Fear & McRoberts (1993, 1995)

† estimated for this study; ‡ assumed to be clean sand (CS)

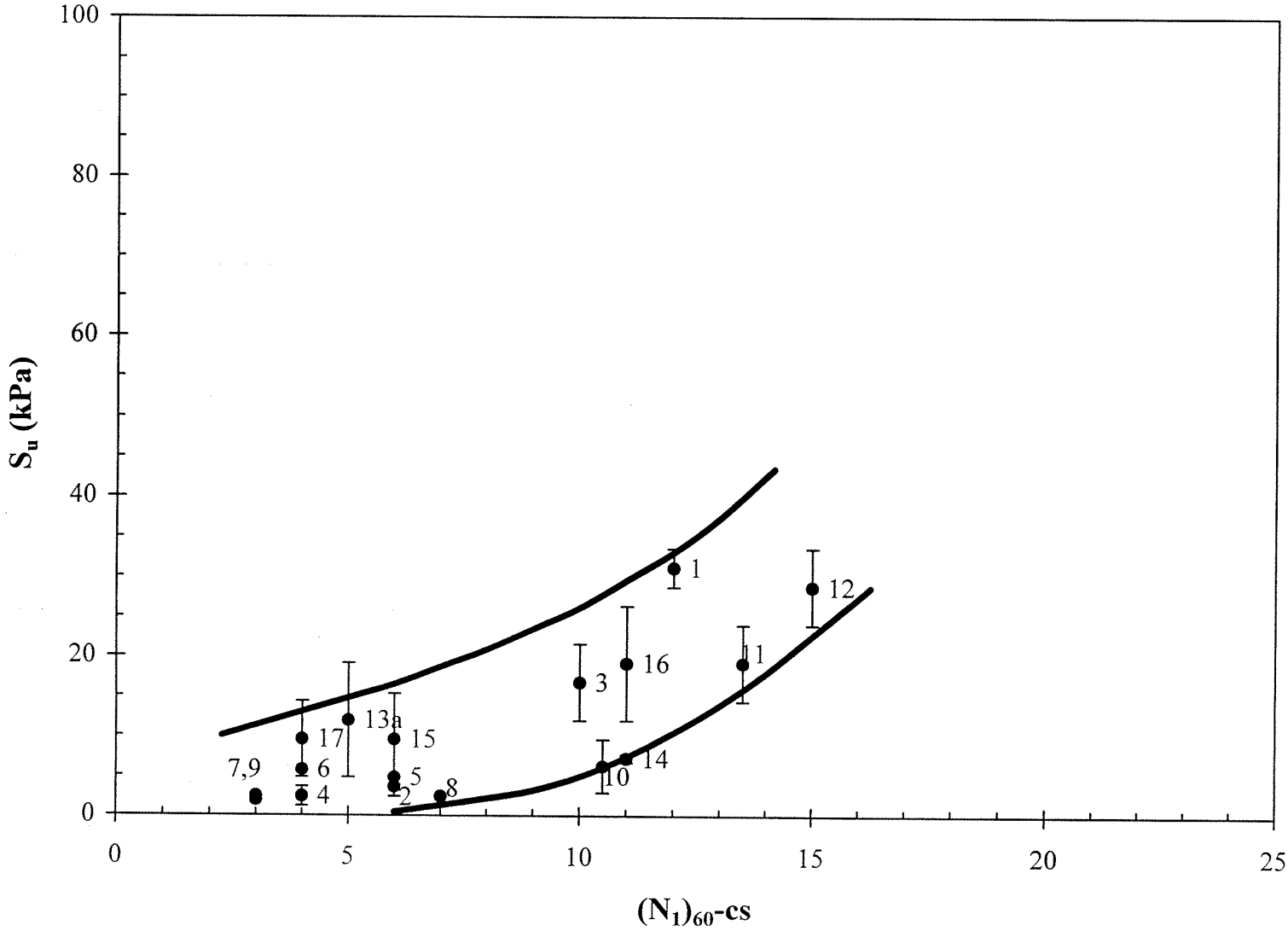

Figure 1. Relationship between clean sand equivalent SPT blowcount, $(N_1)_{60}$-cs, and undrained residual strength (S_u) from case histories (after Seed and Harder, 1990).

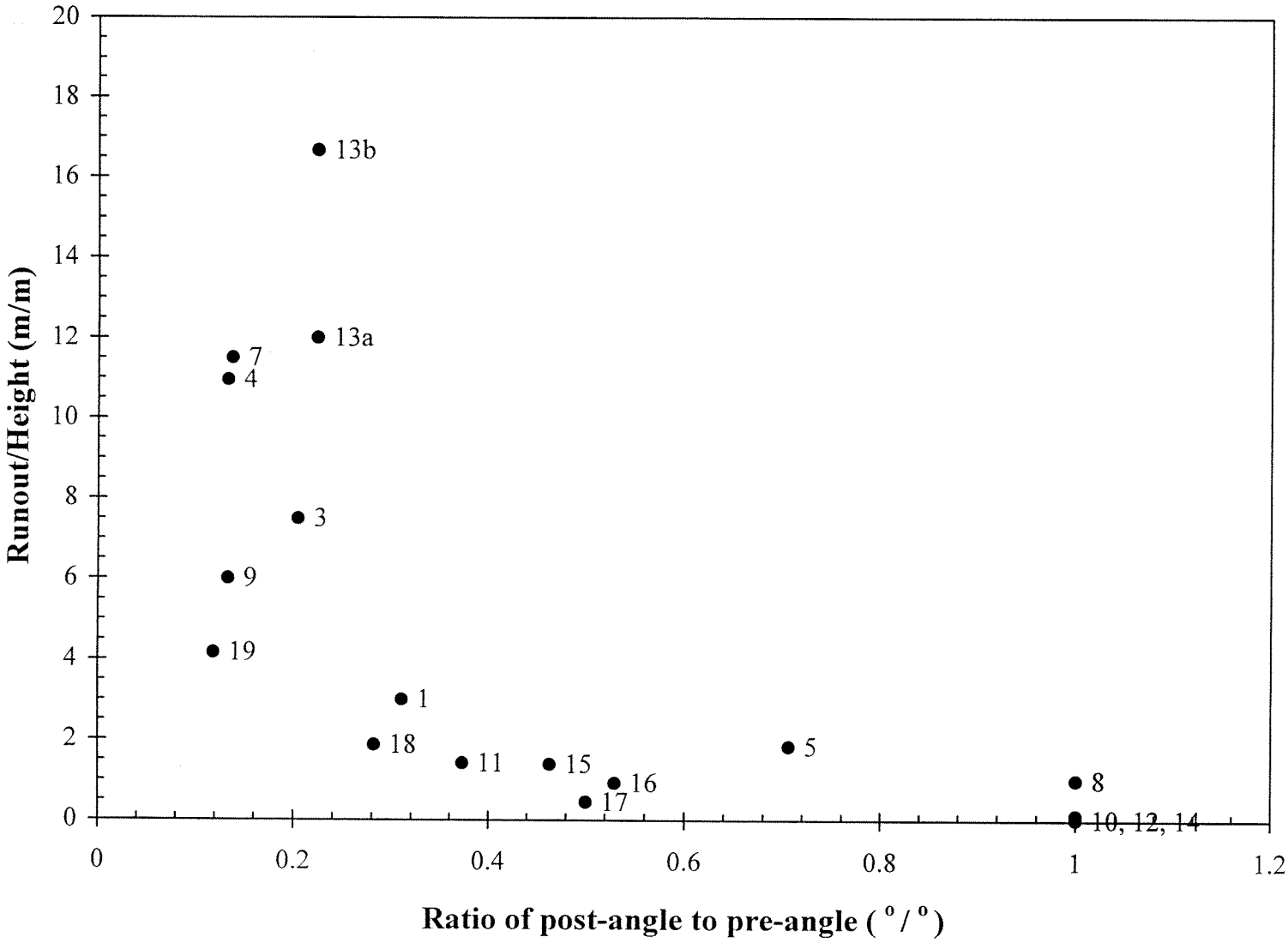

Figure 2. **Case histories from Seed and Harder (1990) and Stark and Mesri (1992) plotted in terms of relative runout (runout/initial height) and slope angle ratio (ratio of post-failure slope angle to initial slope angle).**

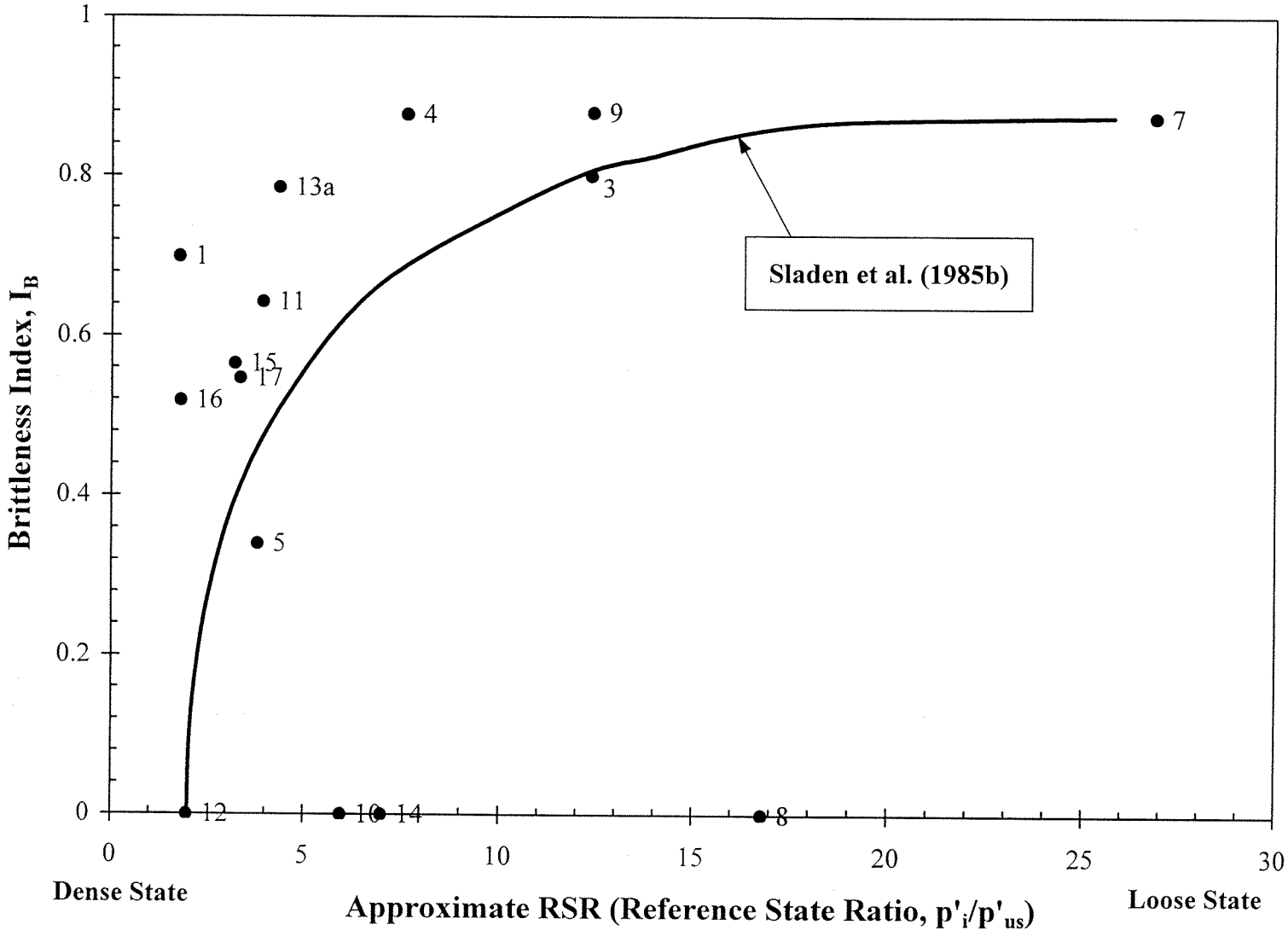

Figure 3. Case histories from Seed and Harder (1990) and Stark and Mesri (1992) plotted in terms of brittleness index versus approximate RSR, with the relationship suggested by Sladen et al. (1985b) shown for comparison.

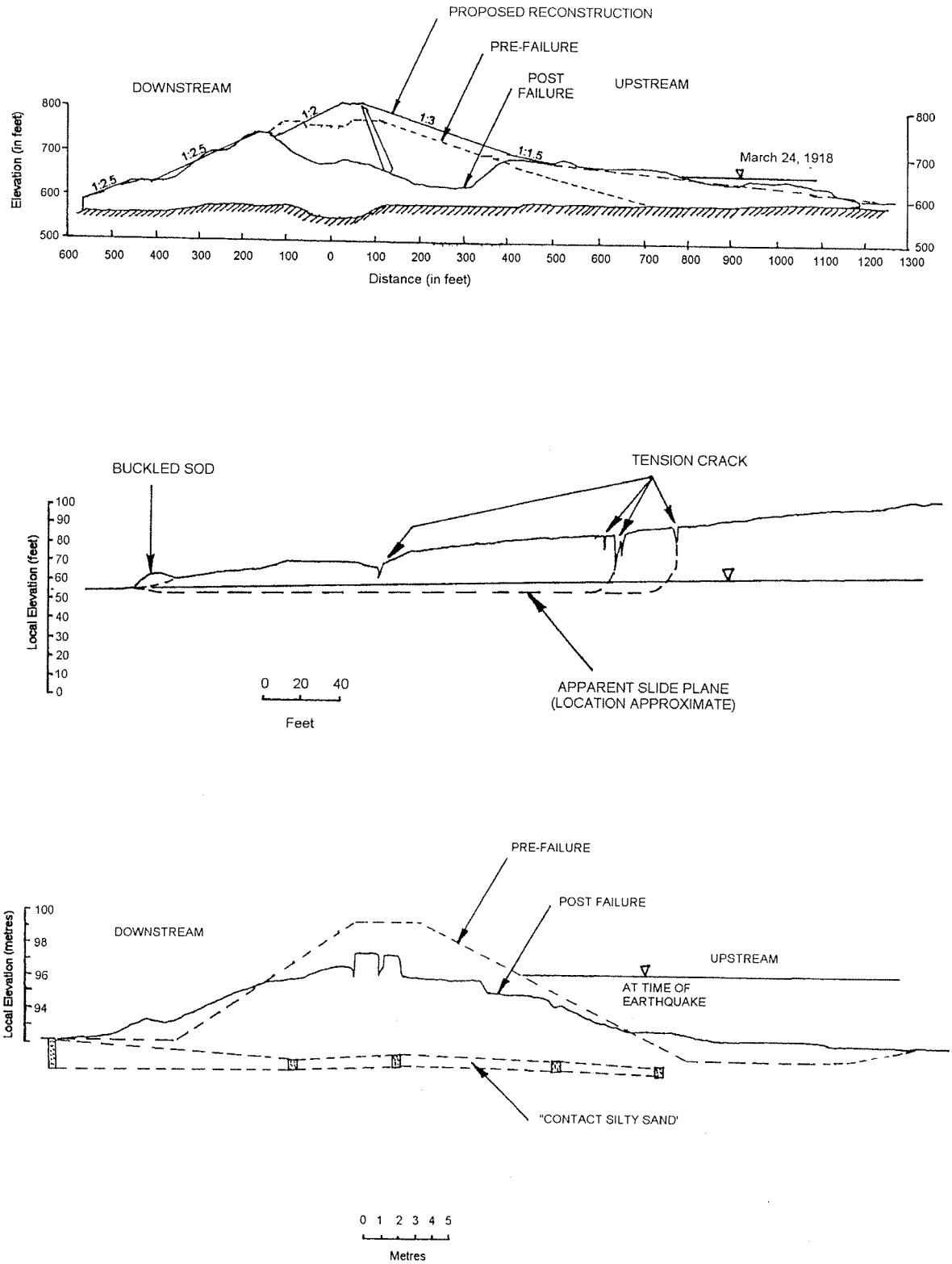

Figure 4. **Pre-failure and post-failure cross-sections for examples of different types of failures: (a) flow: Calaveras Dam (1), after Hazen (1918); (b) lateral spread: Whiskey Springs Fan (14), after Harder (1988); (c) slump: La Marquesa Dam Upstream and Downstream (15 and 16), after De Alba et al. (1988).**

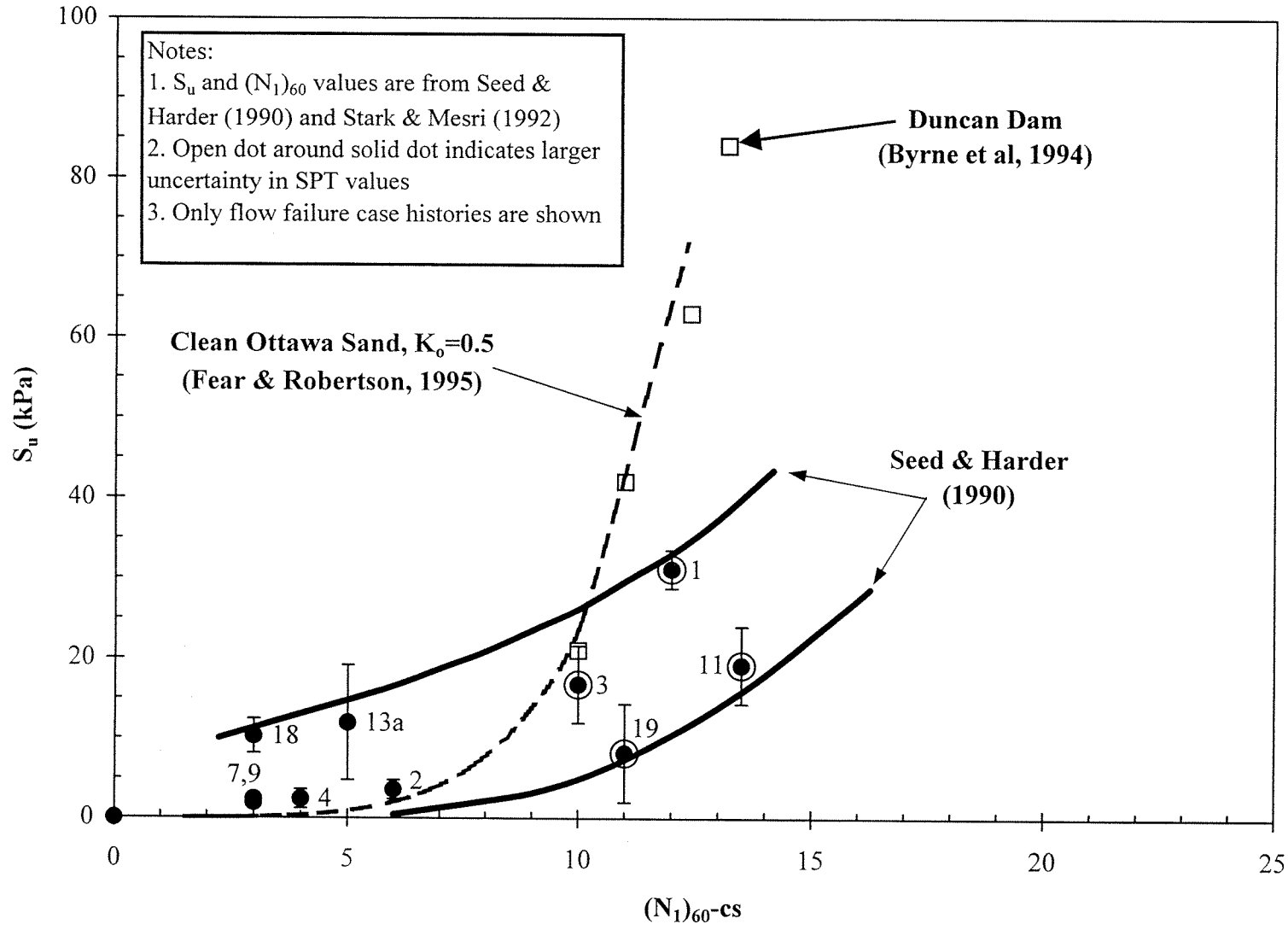

Figure 5. Plot of S_u versus clean sand equivalent SPT blowcount, $(N_1)_{60}$-cs, for those case histories from Seed and Harder (1990) and Stark and Mesri (1992) classified as flow failures, with theoretical clean Ottawa sand line (after Fear and Robertson, 1995) and Duncan Dam (21) results shown for comparison.

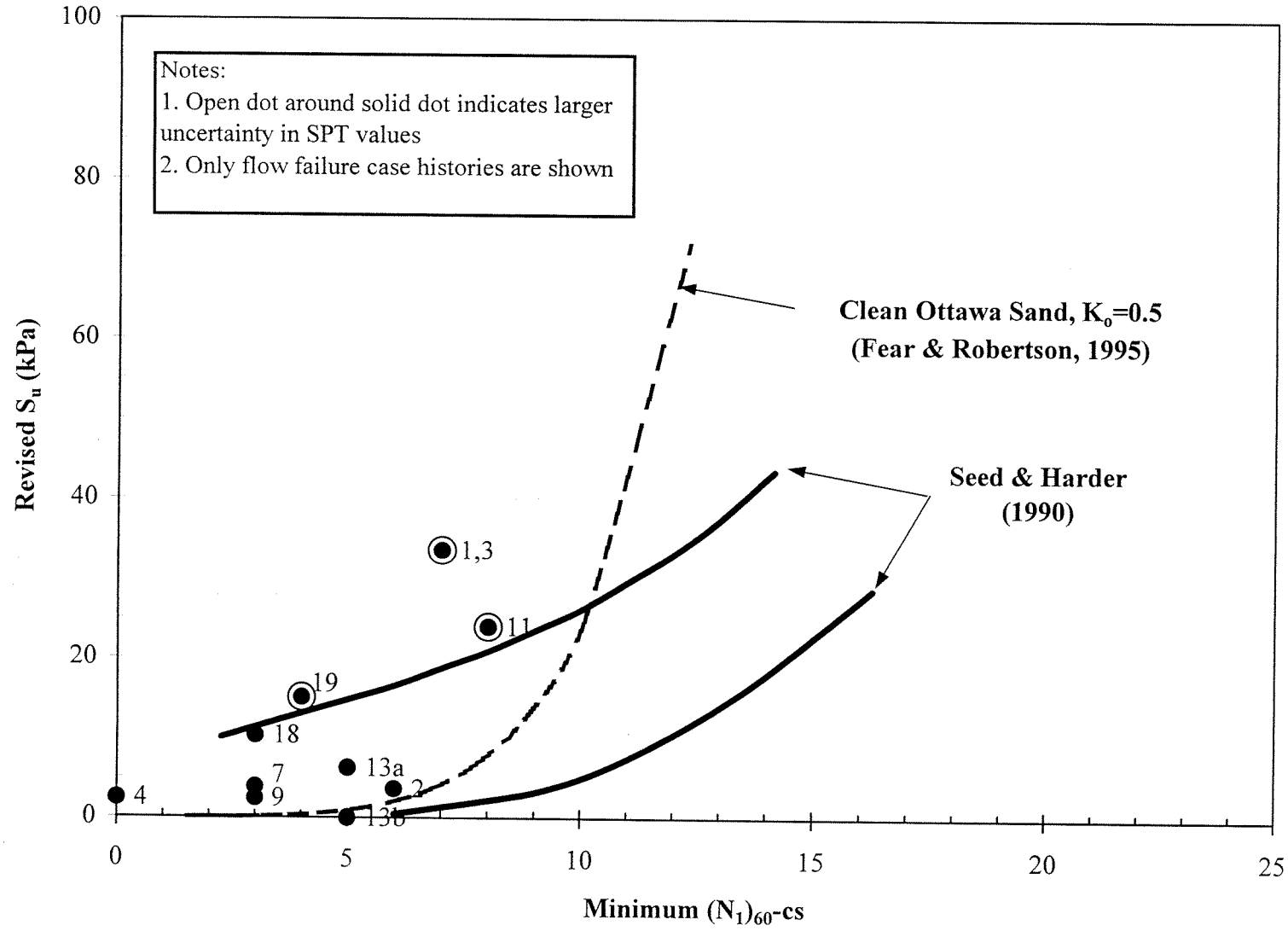

Figure 6. Plot of S_u versus minimum clean sand equivalent SPT blowcount, $(N_1)_{60}$-cs, for those case histories classified as flow failures, with Seed and Harder (1990) lines and theoretical clean Ottawa sand line (after Fear and Robertson, 1995) shown for comparison; note: S_u and $(N_1)_{60}$-cs are the revised values from this study (see Table 9).

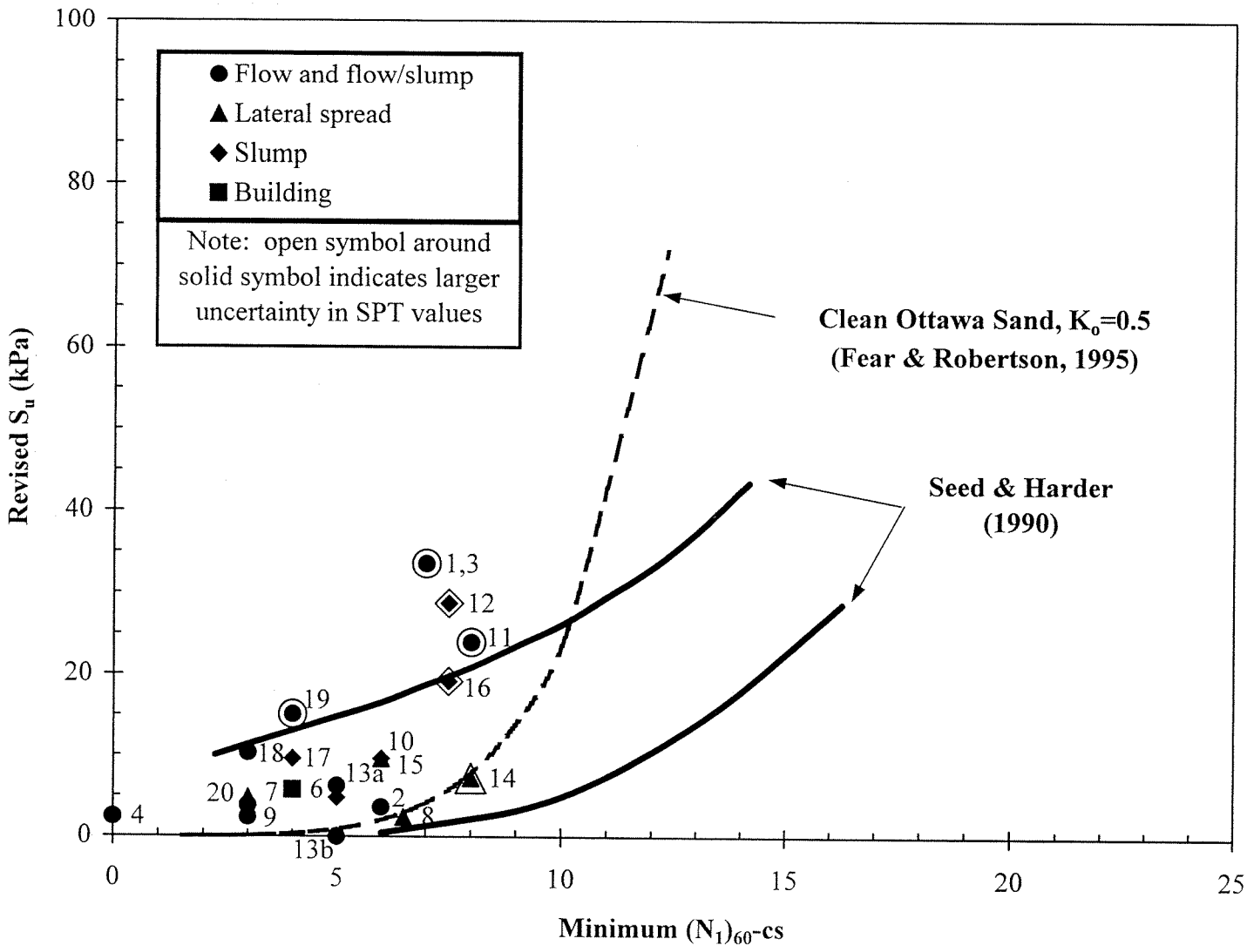

Figure 7. Plot of S_u versus minimum clean sand equivalent SPT blowcount, $(N_1)_{60}$-cs, for all case histories except Lake Merced (5), with Seed and Harder (1990) lines and theoretical clean Ottawa sand line (after Fear and Robertson, 1995) shown for comparison; note: S_u and $(N_1)_{60}$-cs are the revised values from this study (see Table 9).

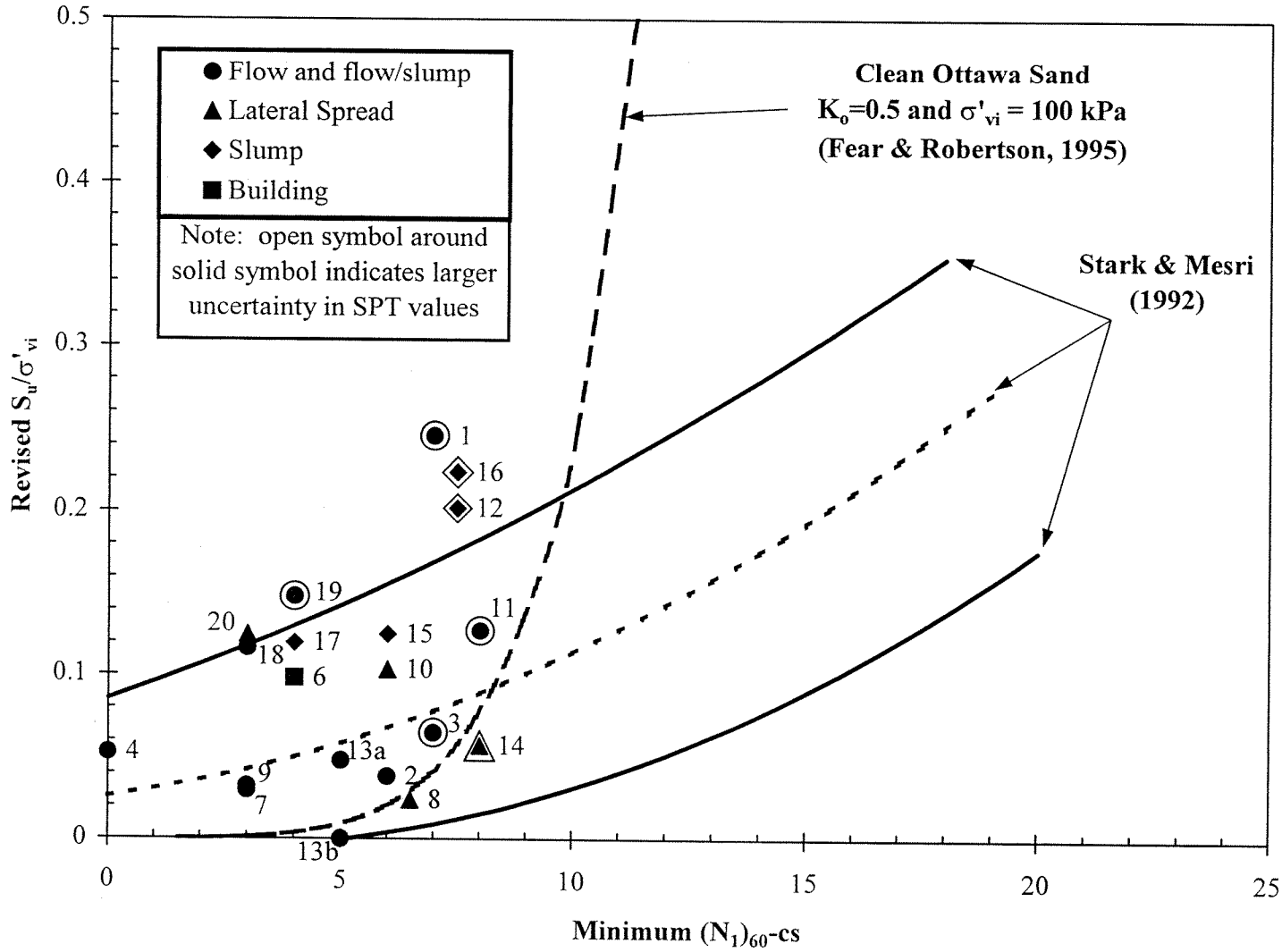

Figure 8. Plot of undrained strength ratio, S_u/σ'_{vi}, versus minimum clean sand equivalent SPT blowcount, $(N_1)_{60}$-cs, for all case histories except Lake Merced (5), with Stark & Mesri (1992) lines and clean sand Ottawa line (after Fear and Robertson, 1995) shown for comparison; note: S_u and $(N_1)_{60}$-cs are the revised values from this study (see Table 9), while values of σ'_{vi} are from Stark and Mesri (1992) (see Table 7).

List of Figure Captions

Figure 1. Relationship between clean sand equivalent SPT blowcount, $(N_1)_{60}$-cs, and undrained residual strength (S_u) from case histories (after Seed and Harder, 1990).

Figure 2. Case histories from Seed and Harder (1990) and Stark and Mesri (1992) plotted in terms of relative runout (runout/initial height) and slope angle ratio (ratio of post-failure slope angle to initial slope angle).

Figure 3. Case histories from Seed and Harder (1990) and Stark and Mesri (1992) plotted in terms of brittleness index versus approximate RSR, with the relationship suggested by Sladen et al. (1985b) shown for comparison.

Figure 4. Pre-failure and post-failure cross-sections for examples of different types of failures: (a) flow: Calaveras Dam (1), after Hazen (1918); (b) lateral spread: Whiskey Springs Fan (14), after Harder (1988); (c) slump: La Marquesa Dam Upstream and Downstream (15 and 16), after De Alba et al. (1988).

Figure 5. Plot of S_u versus clean sand equivalent SPT blowcount, $(N_1)_{60}$-cs, for those case histories from Seed and Harder (1990) and Stark and Mesri (1992) classified as flow failures, with theoretical clean Ottawa sand line (after Fear and Robertson, 1995) and Duncan Dam (21) results shown for comparison.

Figure 6. Plot of S_u versus minimum clean sand equivalent SPT blowcount, $(N_1)_{60}$-cs, for those case histories classified as flow failures, with Seed and Harder (1990) lines and theoretical clean Ottawa sand line (after Fear and Robertson, 1995) shown for comparison; note: S_u and $(N_1)_{60}$-cs are the revised values from this study (see Table 9).

Figure 7. Plot of S_u versus minimum clean sand equivalent SPT blowcount, $(N_1)_{60}$-cs, for all case histories except Lake Merced (5), with Seed and Harder (1990) lines and theoretical clean Ottawa sand line (after Fear and Robertson, 1995) shown for comparison; note: S_u and $(N_1)_{60}$-cs are the revised values from this study (see Table 9).

Figure 8. Plot of undrained strength ratio, S_u/σ'_{vi}, versus minimum clean sand equivalent SPT blowcount, $(N_1)_{60}$-cs, for all case histories except Lake Merced (5), with Stark & Mesri (1992) lines and clean sand Ottawa line (after Fear and Robertson, 1995) shown for comparison; note: S_u and $(N_1)_{60}$-cs are the revised values from this study (see Table 9), while values of σ'_{vi} are from Stark and Mesri (1992) (see Table 7).